METEOR-Berichte

ADRIA LITHOSPHERE INVESTIGATION

ALPHA

Cruise No. M86/3

January 20 - February 04, 2012
Brindisi (Italy) – Dubrovnik (Croatia)

H. Kopp, A. Dannowski, A. Argnani, I. Dasović, I. Dumke, J. Elger, E. Flueh, B. Frey, M.R. Handy, J. Karstens, M. Kordowski, A. Krabbenhoeft, J. Mögeltönder, C. Papenberg, L. Planert, K.-P. Steffen, J. Stipčević, K. Ustaszewski, W. Weinrebe, T. Wiskandt, T. Zander

Editorial Assistance:

DFG-Senatskommission für Ozeanographie
MARUM – Zentrum für Marine Umweltwissenschaften der Universität Bremen

2013

The METEOR-Berichte are published at irregular intervals. They are working papers for people who are occupied with the respective expedition and are intended as reports for the funding institutions. The opinions expressed in the METEOR-Berichte are only those of the authors.

The METEOR expeditions are funded by the *Deutsche Forschungsgemeinschaft (DFG)* and the *Bundesministerium für Bildung und Forschung (BMBF)*.

Editor:
DFG-Senatskommission für Ozeanographie
c/o MARUM – Zentrum für Marine Umweltwissenschaften
Universität Bremen
Leobener Strasse
28359 Bremen

Author:
Prof. Dr. Heidrun Kopp
GEOMAR
Wischhofstraße 1-3,
24148 Kiel

Telefon: +49 431 600 2334
Telefax: +49 431 600 2922
e-mail: hkopp@geomar.de

Citation: H. Kopp, A. Dannowski, A. Argnani, I. Dasović, I. Dumke, J. Elger, E. Flueh, B. Frey, M.R. Handy, J. Karstens, M. Kordowski, A. Krabbenhoeft, J. Mögeltönder, C. Papenberg, L. Planert, K.-P. Steffen, J. Stipčević, K. Ustaszewski, W. Weinrebe, T. Wiskandt, T. Zander (2013) ADRIA LITHOSPHERE INVESTIGATION ALPHA - Cruise No. M86/3 - January 20 - February 04, 2012 - Brindisi (Italy) - Dubrovnik (Croatia). METEOR-Berichte, M86/3, 48 pp., DFG-Senatskommission für Ozeanographie, DOI:10.2312/cr_m86_3

ISSN 2195-8475

Table of Contents

1 Summary

The Adriatic Sea and underlying lithosphere remains the least investigated part of the Mediterranean Sea. To shed light on the plate tectonic setting in this central part of southern Europe, R/V METEOR cruise M86/3 set out to acquire deep penetrating seismic data in the Adriatic Sea. M86/3 formed the core of an amphibious investigation crossing Adria from the Italian Peninsula into Montenegro/Albania. A total of 111 OBS/OBH deployments were successfully carried out, in addition to 47 landstations both in Italy and Montenegro/Albania, which recorded the offshore airgun shots.

In the scope of this shoreline-crossing study, the aim is to quantify the shallow geometry, deep boundaries and the architecture of the southern Adriatic crust and lithosphere and to provide insights on a possible decoupling zone between the northern and southern Adriatic domains. Investigating the structure of the Adriatic crust and lithospheric mantle and analyzing the tectonic activity are essential for understanding the mountain-building processes that underlie the neotectonics and earthquake hazard of the Periadriatic region, especially in the vicinity of local decoupling zones.

Zusammenfassung

Die Adria und die darunterliegende Lithosphäre sind bis heute ein wenig untersuchtes Gebiet im Mittelmeer. Für eine verbesserte Kenntnis der Plattengeometrie wurden im Rahmen der Meteor Ausfahrt M86/3 seismische Daten in der Adria akquiriert. M86/3 formte das Kernstück eines amphibischen Experimentes mit Transekten, die von Italien (Apulien, Gargano) über die Adria bis nach Montenegro bzw. Albanien reichen. Insgesamt 111 OBS/OBH Einsätze wurde erfolgreich durchgeführt und durch 47 Landstationen in Italien bzw. Montenegro/Albanien ergänzt, die die Luftpulser-Schüsse registrierten.

Im Rahmen dieser küstenübergreifenden Studien soll die flache Geometrie sowie die tiefe Architektur der Adriatischen Kruste und Lithosphäre abgebildet werden und mögliche Hinweise auf eine Entkopplungszone zwischen der nördlichen und südlichen Adria untersucht werden. Die Untersuchungen der Krustenstruktur und des lithosphärischen Mantels sowie die Analyse der Tektonik sind wichtige Voraussetzungen, um die gebirgsbildenden Prozesse des peri-Adriatischen Raumes inklusive der Neotektonik und Erdbebengefährdung besser verstehen zu lernen.

2 Participants

Name		Institution
Prof. Dr. Heidrun Kopp	Chief Scientist	GEOMAR
Prof. Dr. Andrea Argnani	Seismics, Bathymetry	ISMAR-CNR
Dr. Anke Dannowski	Seismics	GEOMAR
Iva Dasović	Seismics	Univ. Zagreb
Ines Dumke	Seismics	GEOMAR
Judith Elger	Seismics	TU Berlin
Prof. Dr. Ernst R. Flueh	Seismics	GEOMAR
Bernd Frey	Meteorology	DWD
Prof. Dr. Mark R. Handy	Tectonics	FU Berlin
Jens Karstens	Seismics	GEOMAR
Martin Kordowski	IT	GEOMAR
Dr. Anne Krabbenhoeft	Seismics, Bathymetry	GEOMAR
Dr. Cord Papenberg	Seismics	GEOMAR
Dr. Lars Planert	Seismics	GEOMAR
Klaus-Peter Steffen	Seismics	GEOMAR
Josip Stipčević	Seismics	Univ. Zagreb
Dr. Kamil Ustaszewski	Tectonics	GFZ
Dr. Wilhelm Weinrebe	Bathymetry	GEOMAR
Thorge Wiskandt	Seismics	GEOMAR
Timo Zander	Seismics	CAU

Fig. 2.1: Participants of the METEOR Cruise M86/3.

Participating Institutions:

Christian-Albrechts Universität zu Kiel
Christian-Albrechts-Platz 4
24118 Kiel, Germany

DWD
Deutscher Wetterdienst
Bernhard-Nocht-Straße 76
20359 Hamburg, Germany

Freie Universität Berlin
Malteserstr. 74-100
12249 Berlin, Germany

GEOMAR
Helmholtz-Zentrum für Ozeanforschung Kiel
Wischhofstr. 1-3
24148 Kiel, Germany

GFZ
Helmholtz-Zentrum Potsdam
Deutsches Geoforschungszentrum
Telegrafenberg
14473 Potsdam, Germany

ISMAR-CNR
Institute of Marine Sciences - National Research Council
Via Gobetti 101
40129 Bologna, Italy

Technische Universität Berlin
Straße des 17. Juni 135
10623 Berlin, Germany

University of Zagreb
Horvatovac bb
10000 Zagreb, Croatia

3 Research Program

3.1 Introduction and Aims of the Program

(A. Argnani, M. Handy, H. Kopp, K. Ustaszewski)

The eastern Adriatic margin, where the Adriatic plate is subducted beneath Eurasia to form the Dinaric mountain belt, is one of the most enigmatic segments of the Alpine-Mediterranean collision zone (Fig. 3.1). This is due to an along-strike change in the nature of the plate boundary from a "Albanide-Hellenic" segment in the SE characterized by roll-back subduction of a NE-dipping lithospheric slab and back-arc spreading, to a "Dinaric" segment in the NW dominated by highly oblique (dextral) shortening, no discernible slab and intramontane strike-slip basins. Two of our seismic profiles (P1, P2) and bathymetric maps (Fig. 3.2) are situated near the junction of these segments offshore Montenegro. They are designed to help ascertain how the structure of the Adriatic lithosphere is related to these along-strike differences in collisional geometry and kinematics. The third profile (P3) is oriented NW-SE across a zone of enhanced seismicity that transects the Adriatic plate from the Gargano Peninsula (Italy) to Dubrovnik (Croatia) and is possibly related to ongoing fragmentation of the Adriatic lithosphere. The offshore coastal areas we have studied include numerous sites of instrumental and historical earthquakes with risk for the local population.

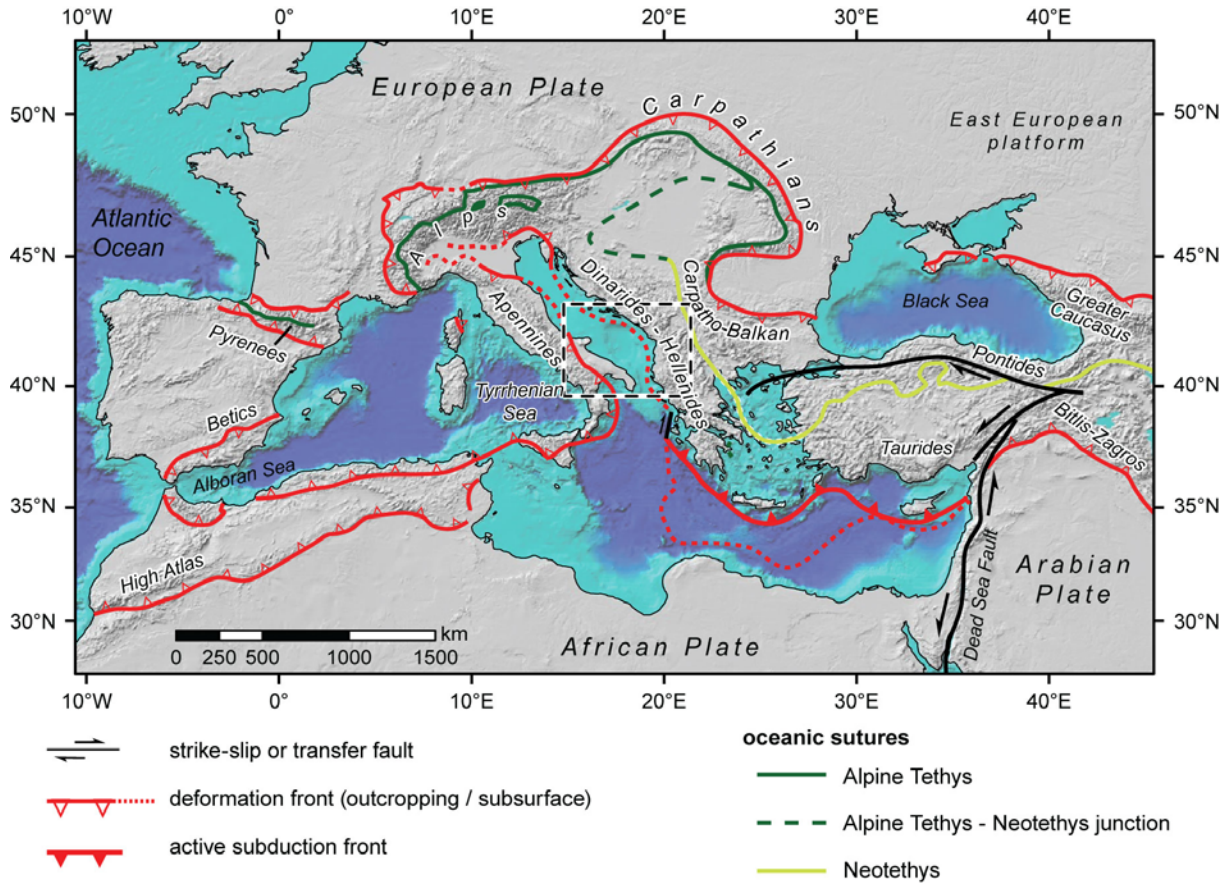

Fig 3.1: Major tectonic elements and topographic relief of the Alpine-Mediterranean area, with dashed box outlining our study area across part of the Adriatic-Europe plate boundary. Thick red lines indicate convergent plate boundaries with subduction direction (barbs on upper plate) determined by the coincidence of orogenic zones with slab images from global tomographic models. The transition from oceanic subduction along the Hellenic arc to continental collision along the eastern margin of the Adriatic Sea occurs along offshore Albania (figure modified from Ustaszewski et al. 2008). The exact location of the plate boundary on the Balkan Peninsula is disputed.

This study therefore addresses the following first-order questions:

- What is the deep structure of the Adriatic plate? Do inherited Mesozoic and Cenozoic platforms and basins coincide with along-strike changes in the geometry and kinematics of the active plate boundary?
- How deep is the Moho beneath the Adriatic platform and does its topography vary along the plate boundary? Does its geometry in the study area reflect the northwestern termination of the deep-reaching Hellenic slab?
- What is the geometry of the deformation front along the Adria-Europe plate boundary? Does it change along strike and can such changes be related to onshore structures of the Dinarides?
- Can an active decoupling zone be imaged between the northern and southern parts of the Adriatic microplate in this area? Such a fault zone has been proposed in recent neotectonic studies based on the coincidence of local seismicity with measured changes in the convergence rate. Characterizing this potential is an important component of improving the assessment of seismic hazard in the region.

To shed light on these issues, we obtained seismic and hydro-acoustic images of the present-day architecture of the Adriatic crust, including the wedge of continental material that is accreted to the upper European Plate along the offshore front of the Dinaric orogen. This involved the acquisition of refraction seismic data with ocean-bottom hydrophones (OBH) and ocean-bottom seismometers (OBS) along two transects (P1, P2) that extended from Apulia (Brindisi) and the Gargano Peninsula to their meeting point near the Montenegro-Albania border, where they continued onshore with seismometers deployed along a transect from the coast of Montenegro into the mountains of northern Albania. This amphibious approach provided new coverage of the transition between the Adriatic basin and the Dinaric fold-and-thrust belt. Post-cruise work is foreseen to integrate seismological data from the existing national onshore networks, as well as existing geological data on the neotectonics of the External Dinarides.

3.2 Tectonic Setting of the Adriatic Sea and Surrounding Collision Zones

(A. Argnani, M. Handy, K. Ustaszewski)

Current plate tectonic activity in the eastern Adriatic Sea must be regarded against the background of a long history of convergence between the European, African and Adriatic Plates. In the Dinarides, this convergence began with Middle Jurassic to Late Cretaceous closure of the Neotethyan ocean, as documented onshore by large ophiolitic nappes along the length of the Balkan Peninsula (Fig. 3.2). Suturing of this ocean ended in Late Cretaceous-early Paleogene time (Pamić 1993, 2002; Schmid et al. 2008; Ustaszewski et al. 2010) and subsequent collision involving nappe stacking and folding migrated from NE to SW, i.e., from internal to external parts of the orogen. This was accompanied by Late Cretaceous to Miocene magmatism (Yanev and Bardintzeff 1997; Cvetković et al. 2004), extension and basin formation (e.g. Dumurdzanov et al. 2005; Burchfiel et al. 2008, Copley et al. 2009) that also migrated from internal to external

parts, suggesting that the convergent plate boundary retreated to the SW away from the Neotethyan oceanic suture (Burchfiel et al. 2008, Schefer et al. 2011). The development of the SE part of the Dinarides is closely tied to the evolution of the Hellenic arc-trench system in the Aegean area, where roll-back subduction and both arc-parallel and arc-normal extension have lead to the formation of metamorphic core complexes containing the attenuated remains of the Paleogene nappe stack (Lister et al. 1984, Jolivet and Brun 2009).

The continuation of the Hellenic arc-trench subduction system into the Dinaric fold-and-thrust belt is marked by a transition from oceanic to continental subduction that coincides with the Kefalonia transform fault (Figs. 3.1-3.2). Yet, roll-back subduction and back-arc extension appear to extend beyond this transition as far northwest as the NE-SW trending Scotari-Pec Fault in northern Albania (Fig. 3.2, Burchfiel et al. 2008), on a line with where continental Adriatic lithosphere enters the subduction zone and GPS studies suggest ongoing convergence at a rate of 4–5 mm/a (Grenerczy et al. 2005; Bennett et al. 2008; D'Agostino et al. 2008; Caporali et al. 2009).

Defining the Adriatic microplate (termed Adria), particularly along its active Dinaric margin, remains an elusive endeavour, because seismic activity at its boundaries is diffuse **(**Wortmann et al. 2001, Vannucci et al. 2004, Fig. 3.3) and because the gradients in recent plate motion vectors are low and poorly constrained (Figs. 3.4-3.6). Since its individuation from the Africa plate in Mesozoic time (e.g., Biju-Duval et al. 1976, Channell and Horvath 1976), Adria has shrunk considerably in areal extent and moved sporadically with respect to all of its surrounding plates, even up to the present time (Handy et al. 2010 and references therein). Today, Adria is a block of mostly continental lithosphere which forms a rigid indenter in the Alps (e.g., Schmid et al. 2004), but which has been largely subducted to the west and northeast during soft collision, respectively, along the Apennines (e.g., Facenna et al. 2004) and Dinarides (Moretti and Royden 1988). Most of the stable (i.e., unaccreted) part of the Adriatic lithosphere lies submerged beneath the Adriatic Sea, with only modest onshore exposures in Apulia, along the eastern and northern coasts of Italy, the Istrian Peninsula of Slovenia and the Sazani Peninsula of central Albania (Fig. 3.2). The southern boundary of Adria towards Nubia is not well defined and may not actually exist, at least in the sense of a sharply defined boundary.

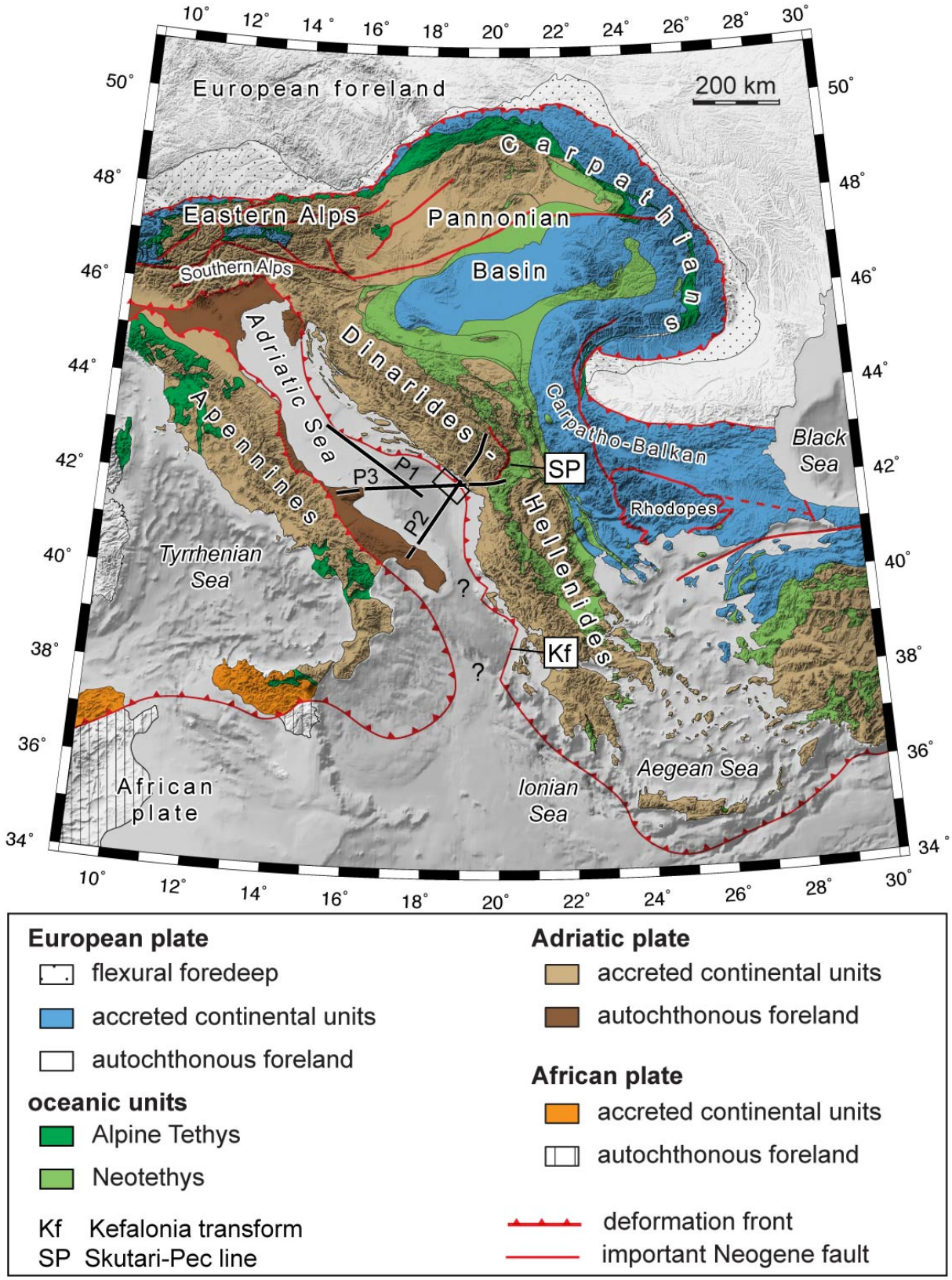

Fig. 3.2: Detailed tectonic map of the Adriatic area with the location of seismic profiles P1, P2 and P3. Small box shows areas mapped hydro-acoustically in this study. Thick red lines indicate convergent plate boundaries with subduction direction (barbs on upper plate) determined by the coincidence of orogenic zones (map modified from Schmid et al. 2008) with slab images from global tomographic models (Bijwaard & Spakman 2000, Piromallo & Morelli 2003). SP = Scotari-Pec Fault, KF = Kefalonia Fault (see text for explanation).

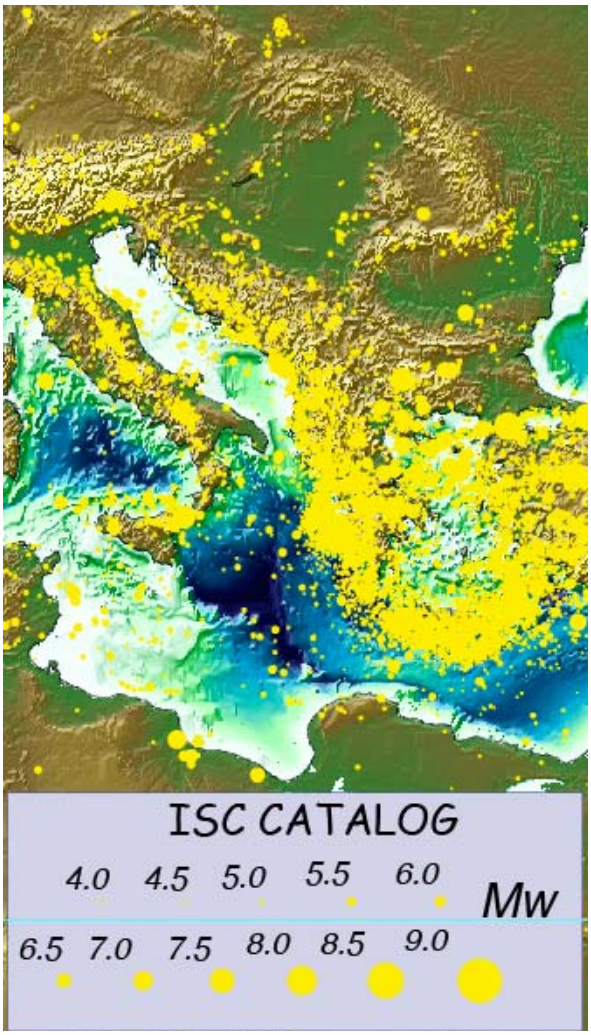

Fig. 3.3: Seismicity map of the Adriatic area for earthquakes up to 2004 (modified from Fig. 3 in Vannucci et al. 2004).

Three basic kinematic models, all based on earthquake slip vectors and geodetic data, have been proposed to account for the highly complex tectonics of the region:

(1) Adria is a distinct microplate that moves independently of Eurasia and Nubia (Anderson and Jackson 1987);
(2) Adria is fragmented into two or more pieces which each move independently of both Eurasia and Nubia (Fig. 3.5, Battaglia et al. 2004; Grenerczy et al. 2005)
(3) The northern part of Adria has become part of the Eurasian plate, whereas southern part represents a promontory of Nubia (Oldow et al. 2002).

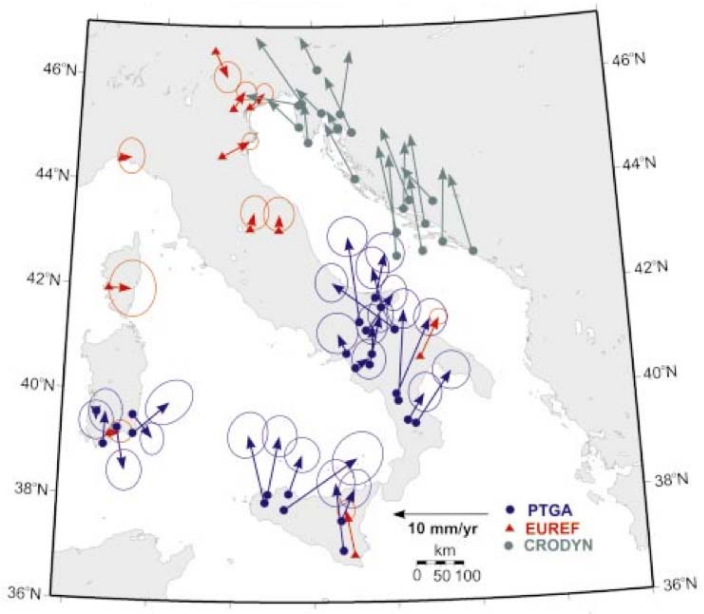

Fig. 3.4: GPS velocities (ellipses are 95% confidence) interpreted to show the fragmentation of Adria into separate subblocks or microplates (from Oldow et al. 2002).

A decoupling zone between the northern and southern parts of Adria (Fig. 3.5), the Gargano-Dubrovnik Zone, was proposed to accommodate a purported along-strike change in the plate convergence vectors between Adria and Europe from c. 1-2 mm/a in the NW to 4-5 mm/a in the SE (Oldow et al. 2002; Grenerczy et al. 2005; D'Agostino et al. 2008). However, the distribution of earthquake epicenters is ambiguous (Fig. 3.6) and does not really necessitate a decoupling zone (Babbucci et al. 2004), which thus remains controversial. If such a

decoupling zone indeed exists, it would represent a new plate boundary in the center of southern Europe.

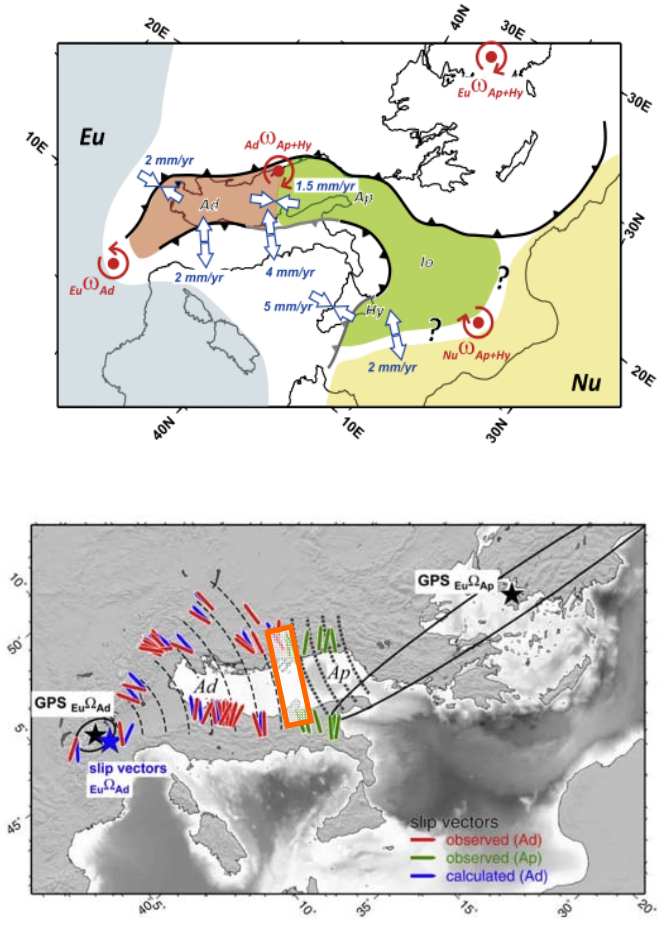

Fig. 3.5: Upper panel: Seismo-tectonic sketch of the microplate subdivision of the Adriatic Promontory into the northern Adriatic and southern Apulian microplates. Lower panel: Earthquake slip vectors around Adria and small circles (dashed lines) around the GPS poles of rotation (black stars) show the motion direction of Adria and Apulia relative to Eurasia. The orange rectangle indicates the position of the postulated Gargano-Dubrovnik decoupling zone (modified from D'Agostino et al. 2008).

The deformation front of the presently active, convergent plate boundary is located along the Adriatic coast in Croatia and Albania as indicated, by earthquakes (e.g. Console and Favali 1981; Benetatos and Kiratzi 2006) and geodetic evidence (Grenerczy et al. 2005; Bennett et al. 2008; D'Agostino et al. 2008; Caporali et al. 2009). (Fig. 3.6). This seismicity has included one of the largest instrumentally recorded earthquakes in Europe, the 1979 Mw=7.1 Montenegro event.

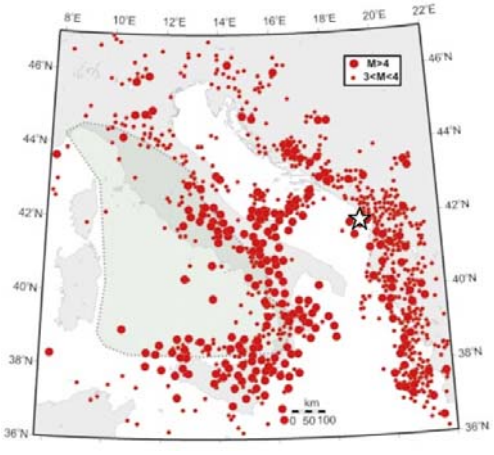

Fig. 3.6: Earthquake epicenters from US Geological Survey (1986-1998) and location of the 1979 Montenegro earthquake (Mw=7.1) indicated by the star (modified from Oldow et al. 2002). The Gargano-Dubrovnik Zone is a postulated decoupling zone between northern and southern parts of the Adriatic plate beneath the Adriatic Sea. Its trace corresponds to a band of enhanced seismicity crossing Adriatic Sea from central Italy to southern Croatia.

Little is known about the deep structure of the Dinaric collision zone. Regional seismic tomography indicates an inclined high-velocity zone down to a depth of ~150 km beneath the Dinarides (Fig. 3.7, Bijwaard and Spakman 2000, Piromallo and Morelli 2003). This anomaly has been interpreted as subducted Adriatic lithosphere (Wortel and Spakman 2004) that is located ~200 km west of the presumed Adria-Eurasia plate boundary that is marked by an oceanic suture zone (Ustaszewski et al., 2010). The crustal structure and Moho are poorly resolved and dominated by large seismic transition zones (Venisti et al. 2005) that are not

obviously linked to the tectonic structures observed at the surface. The neotectonic processes as well as the origin and structure of the Dinaric orogenic belt cannot be deduced unequivocally without detailed knowledge of the underthrusting Adriatic microplate(s) (Šumanovac et al. 2009; Herak 1991).

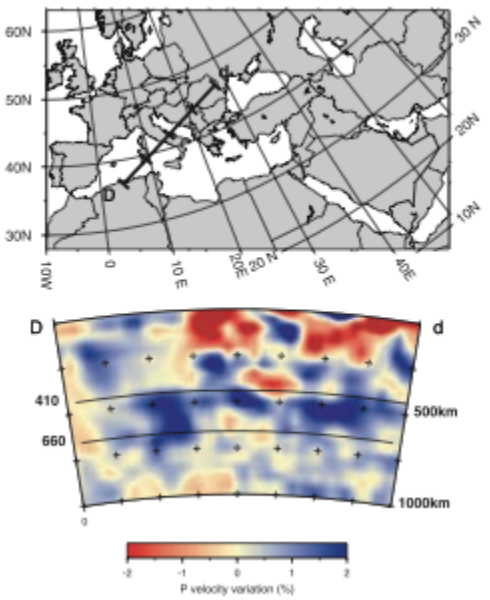

Fig. 3.7: P-wave tomography in a cross section of the Adriatic Plate and neighboring regions based on teleseismic data (from Piromallo and Morelli 2003).

The interior of the Adriatic plate remains unresolved as well, primarily because regional models based on geological and geodetic information are developed from onshore exposures of the Adriatic block adjacent to the surrounding orogenic belts (Fig. 3.2), rather than from the actual core of the plate where data are sparse or lacking. Uncertainty regarding the crustal structure and lithospheric geometry of Adria results from the fact that most of it is submerged beneath the Adriatic Sea and thus only accessible with marine geoscientific approaches.

Crustal thickness estimates for the southern Adriatic Sea are based on gravity interpretations or earthquake analysis using stations located along the rim of the Adriatic Plate (e.g., tomograms in Figs. 3.7-3.8). For the past 30 or more years, there have been no deep-penetrating crustal-scale marine seismic profiles collected in the study area. Seismic reflection data, which imaged the top of the carbonate sequence has been collected from the Italian side of the southern Adriatic Sea (Nicolai and Gambini 2007), but no deep penetrating data exists for the central and southeastern Adriatic Sea. Industrial and Italian ministerial shallow- and deep-seismic profiles in the Central Adria Sea west and north of our study area were referred to recently by Scisciani and Calamita (2008).

Measuring the structure of the Adriatic crust and lithospheric mantle and analyzing the seismic activity are essential for understanding the mountain-building processes that underlie the neotectonics and earthquake hazard of the Periadriatic region, especially in the vicinity of local decoupling zones. In chapter 5.2.2, we provide new tomographic images from active-source seismology that yield insight into the crustal structure of Adria.

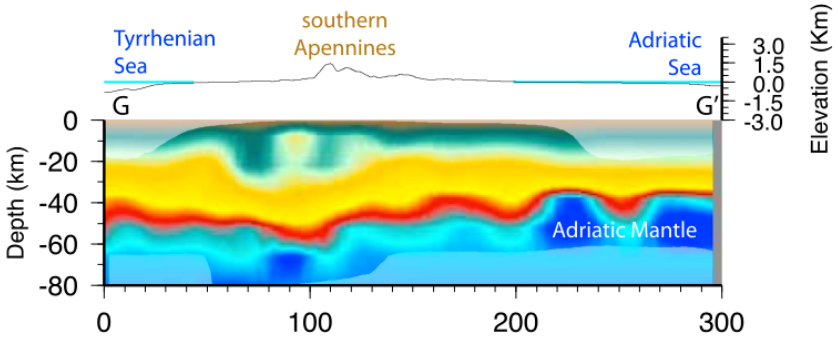

Fig. 3.8: Tomographic image of the Italian lithosphere and western Adria. (from Di Stefano et al. 2009). The cross section trends SW-NE at c. 41°N and passes through the city of Naples.

4 Narrative of the Cruise

(H. Kopp)

The cruise M86/3 started on January 20, 2012 in Brindisi, Italy. An international group of scientists from Croatia, Italy, Switzerland, Austria and Germany embarked on FS METEOR at 09:00 20.01.12- After a short transit of two hours we began our studies with the deployment of a sound-velocity profiler. The station was also used to test our release units. Thereafter, we began deploying 36 Ocean Bottom Seismometers and Hydrophones (OBS/OBH) along profile P02 at an average spacing of 2.7 nm; all 36 instruments (OBH01 to OBS36) were deployed within 18 hours. Subsequently, an airgun array consisting of 6 G-gun clusters with a total volume of 80 l was fired across the 98 nm long spread of seismometers with a trigger interval of 60 s at the ship's average speed of 4.0 kn, resulting in a shot spacing of 100 m. In addition, an 8-channel streamer was deployed. Prior to shooting, communication with our partners onshore in Italy and Montenegro verified that all onshore stations were ready for recording. Shooting terminated at 13:00 on 23.01.12 and subsequently instruments were recovered. The cruise track is displayed in Figure 4.1. The last station (OBS36) along track remained on the seafloor and an additional OBS (OBS37) was deployed between the end of the profile and the shore of Montenegro, approximately 1.5 nm from the coast.

Due to adverse weather conditions with gales up to 12 Bft in the central Adria, R/V METEOR remained close to the Montenegro shore where wind and wave conditions were calm. We commenced the seafloor mapping survey in the source region of the 1979 Montenegro M_w 7.1 earthquake at 17:00 24.01.12 and continued the swath mapping until the next morning. At 05:30 25.01.12 we deployed two additional OBS (OBS38 and OBS39) off the coast of Montenegro and subsequently used all airgun clusters to shoot a 20 nm long coast-parallel profile at a speed of 4.5 kn. The four instruments on the seafloor during shooting (OBS36 to OBS39) were deployed to minimize the gap between the offshore stations along P02 and the onshore seismometers deployed in extension of our track in Montenegro, which were installed to record the offshore airgun shots. The coast parallel profile P04 was geared to provide a fan shooting geometry for the onshore seismometers and to yield across-strike information for P02. Shooting of P04 terminated at 15:30 25.01.12 and the four remaining OBS stations were successfully recovered. We continued the swath mapping activities at 17:30 25.01.12 until the next morning, when instrument deployment at an average spacing of 3.6 nm along P03 commenced. All 36 instruments (OBS40 to OBH75) were deployed starting at 09:00 26.01.12 offshore Albania and heading back towards Italy, where the profile terminates after 130 nm offshore Gargano Peninsula. After deployment of the last station at 03:00 27.01.12 we confirmed that the onshore stations were set up for recording. Profile P03 is extended onshore on the Gargano promontory and into northern Albania, where land stations have been installed along strike of the offshore profile to record the airgun shots. Shooting started at 09:00 27.01.12 as we headed back towards the Montenegro-Albania coast. The streamer was deployed on the profile. Shooting was conducted at an interval of 60 s at a speed of 4.5 kn on average and terminated at 12:30 28.01.12 near the coast of Albania. As the last station was deployed in water depth of less then 60 m, we recovered the station using METEOR'S speedboat. OBS 68 responded to our transducer signal, however, could not be spotted on location. After ~2.5 hrs of search, the instrument could be

retrieved; it had already released on Jan. 27, approx. 20:00. This was not due to erroneous programming of the time release, but must rather be attributed to a malfunction of the release

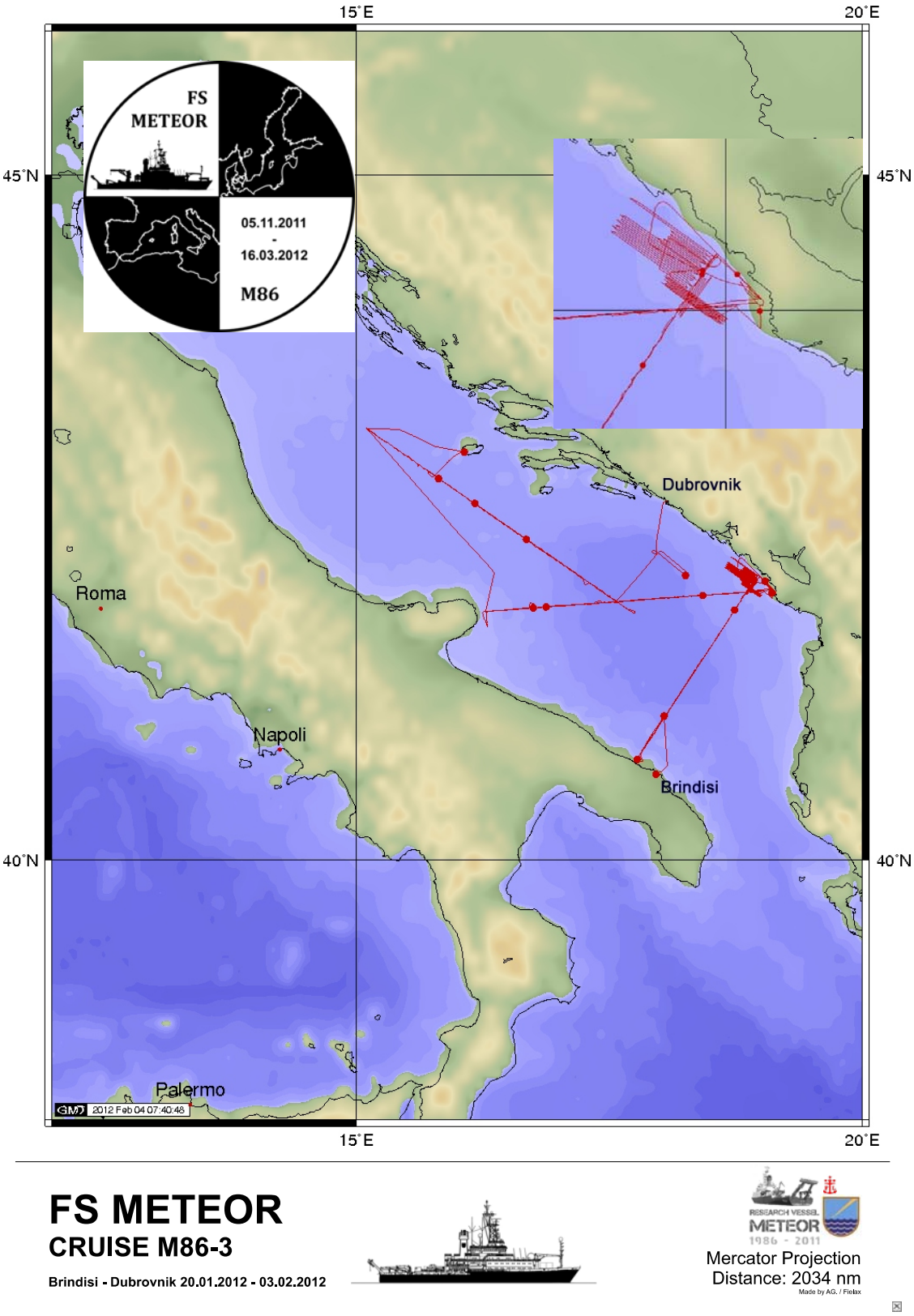

Fig. 4.1: Cruise track M86/3.

unit. All other stations were recovered successfully by 20:30 29.01.12 so that we could start our transit to the northern termination of Profile P01. P01 is a NW-SE trending seismic profile with a total extension of 165 nm and an instrument spacing of 3.6 nm. Deployment of OBS76 – OBH111 started at 05:00 30.01.12 and was terminated after 19 hours. Airgun deployment at 01:30 31.01.12 was conducted with wave heights reaching 2 m and proved difficult on the portside, where the use of a crane is not possible because R/V METEOR's deck crane does not reach far enough. The streamer was deployed in addition. The wind and wave conditions improved during the early morning hours of 31.01.12, but wind and waves increased during the night. Winds gusts of up to 90 kn are expected in our working area on 01.02.12. We were thus forced to recover the airguns and streamer at 22:30 31.01.12 after having shot over OBS82. We subsequently sailed to the Island of Vis and anchored in the Bay of Komiza to wait for improving weather conditions. We departed from here at 02:00 02.02.12 to start our transit back to P01 for instrument recovery. All instruments were recovered between 06:00 02.02.12 and 08:00 03.02.12 and all had recorded successfully.

The weather forecast predicted winds of >60 kn for our transit to Dubrovnik. We were thus forced to cancel the initially planned additional bathymetric survey for 03.02.12 and sail directly to port, arriving 14 hours ahead of schedule. In the evening of 03.02.12 at 18:00 the pilot entered the R/V METEOR, and soon after R/V METEOR berthed in Dubrovnik, terminating cruise M86/3.

5 Preliminary Results

5.1 Bathymetry

(A. Argnani, M. Handy, W. Weinrebe, K. Ustaszewski)

Two multibeam systems are available onboard R/V METEOR for bathymetric mapping of the seafloor: a KONGSBERG EM122 for deep-water mapping and a KONGSBERG EM710 for shallow water.

The EM122 system is a deep-water multibeam echosounder that provides accurate bathymetric mapping of the seafloor. Basic components of the system are two linear transducer arrays in a Mills cross configuration with separate units for transmitting and receiving. The nominal sonar frequency is 12 kHz with an angular coverage sector of up to 150° and 256 beams per ping. The emission beam is 150° wide across track, and 1° along track direction. The reception is obtained from 256 beams, with widths of 2° across track and 20° along track. Thus, the actual footprint of a single beam has a dimension of 1° by 2°. Achievable swath width on a flat bottom will normally be up to six times the water depth depending on the character of the seafloor. The angular coverage sector and beam pointing angles may be set to vary automatically with depth according to achievable coverage. This maximizes the number of usable beams. The beam spacing can be chosen to be equidistant or equi-angle at the seafloor, in addition a "high-density-equidistant" mode is available. Using this mode 432 independent depth values (soundings) are obtained perpendicular to the track for each ping. Using the 2-way-travel-time and the beam angle known for each beam, and taking into account the ray bending due to refraction in the water column by sound speed variations, depth is calculated for each beam. A combination of amplitude (for the central beams) and phase (slant beams) is used to provide a measurement accuracy that is practically independent of the beam-pointing angle.

The EM710 of R/V METEOR is a 1° by 1° broadband multibeam echosounder operating in the 70 kHz to 100 kHz band. Maximum water depth of the system is up to 1500 m to 2000 m, but the most efficient depth range for the EM710 is less than 500 m. In this depth it has a better resolution and a slightly wider swath than the EM122. For greater depths, the EM122 is the system of choice. Basic principles are almost identical to those of the EM122, with differences including the higher sonar frequency (which also means considerably smaller transducer arrays), a beam footprint of 1° by 1°, a total swath width of up to 140° (instead of 150°) and the number of 400 soundings per ping (instead of 432). Common to both systems is the "dual swath" technology, which means that two pings (rather than one) are simultaneously transmitted and recorded, one slightly tilted forward and one backward, thus enabling a denser bottom coverage along track, or allowing for a higher survey speed. So independent depth values are achieved with each record 864 (EM122) resp. 800 (EM710). Both systems also apply CW (continuous wave) pulses in shallow modes and FM pulses in deep modes. FM or "chirp" pulses transmit more energy to the water, thus enabling greater ranges of the beams, in turn leading to better across-track coverage of the seafloor, particularly at greater depths. On the other hand, systems applying FM pulses demand additional features of the motion reference unit because the acoustic signals travel a longer time through the water while the vessel is moving. Consequently, the motion sensor of R/V METEOR was recently upgraded to a Seapath-300, an inertial motion-reference unit, which is augmented by GPS-signals.

Multibeam Data Processing

Processing multibeam data involves two steps: a profile–oriented processing followed by area-based processing. The former requires checking navigational data, interpolating missing navigational values, calculating water depth in order to determine the location of the beam swaths by ray-tracing through the water-column (taking into account the sound velocity profile) and finally, data cleaning by removing artefacts and erroneous data points. Area-based processing comprises the calculation of a digital terrain model (DTM) and the visualisation of the data. For these purposes, the R/V METEOR is equipped with the NEPTUNE software package from KONGSBERG. However, mainly for easier integration of other data from different systems in various data formats, we processed the multibeam data with the "open source software" packages MB-SYSTEM (Caress and Chayes, 1996) and GMT (Wessel and Smith, 1995).

Interpretation

We carried out the swath bathymetry survey where seismic reflection data had revealed the presence of a broad anticlinal feature that possibly protruded on the sea floor (Fig. 5.1). Subbottom profiles (PARASOUND) were also acquired in addition to bathymetry. A remarkable elliptical feature is present just above the anticline (Fig. 5.2) with its long axis oriented WNW-ESE and dimensions of 6 km long by 2 km wide. It has rather sharp boundaries and a flat top that protrudes about 20 m above the surrounding sea floor (Fig. 5.3). We interpret the very rugged morphology on the top of this protrusion to be due to dissolution (pot holes, crevasses, salt erosion, karst features ?); this morphology is most pronounced on the SE part of the plug, where isolate pinnacles are imaged. The overall morphology of this feature, combined with evidence from seismic reflection and sub-bottom profiles, suggests that it may have originated as a salt plug that forms a spine extruding upward from a host diapir at depth, as observed in the North Sea (e.g., the North Pierce diapir, Davison et al., 2000). In fact, the sub-bottom PARASOUND

profiles clearly show a broad dome-like structure that has a much larger wave length (6-8 km) than the salt plug, comparable to the width of the aforementioned anticline imaged on seismic profiles (Fig. 5.2).

Besides the possible salt plug cropping out at the sea floor, swath bathymetry reveals a broad field of dunes that discontinuously covers an area at least 20 km wide (Fig. 5.4). In spite of the patchy appearance, the crests of the dunes trend rather consistently ENE-WSW. Over the dune field PARASOUND profiles show sedimentary bodies with progradational foresets that are few meters thick (Fig. 5.5). The discontinuous appearance of these dunes is possibly related to sea floor erosion, as suggested by smoothing of dune morphology and truncation of sedimentary strata.

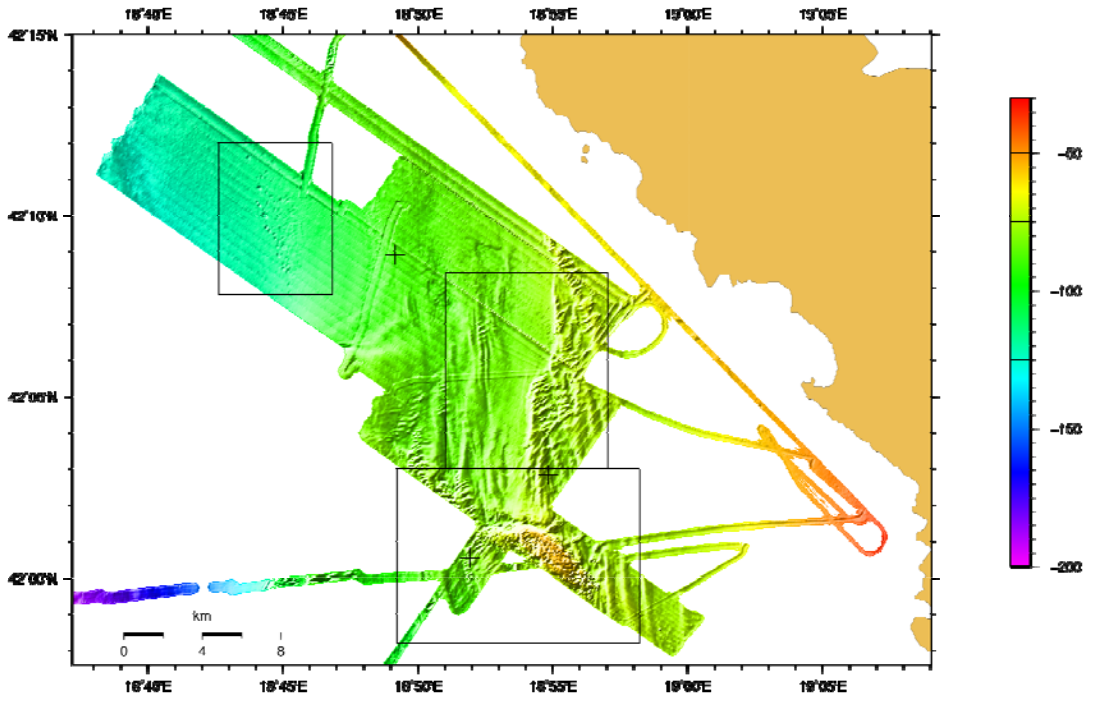

Fig. 5.1: Overview of the bathymetry survey conducted offshore Montenegro. Color scale is in m. Black boxes indicate the location of enlarged maps shown in Figures 5.3 (lower box), 5.4 (central box) and 5.7 (upper box).

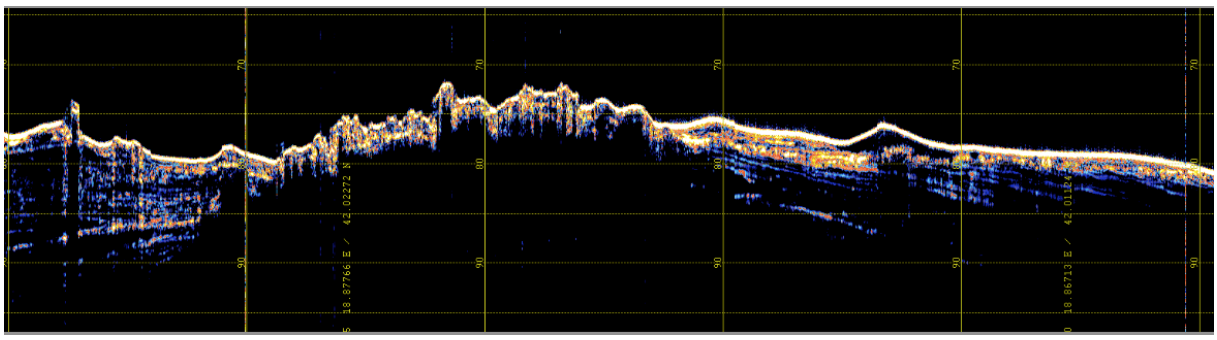

Fig. 5.2: Part of a NNE-SSW-trending PARASOUND profile (c. 6 km long) crossing the "diapir plug" (NNE on left). The strata that flank the "plug" become flatter away from the plug, suggesting that they were deposited during progressive (gradual) doming. Note the finely corrugated top of the "plug", which is quite different from the adjacent sea floor.

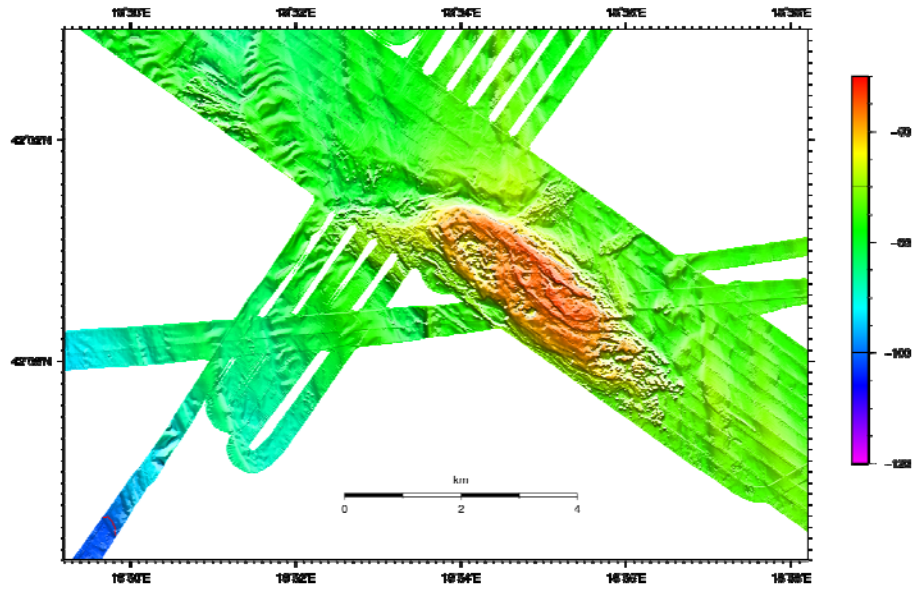

Fig. 5.3: High-resolution bathymetry map of a dome-like structure, which has been identified as a possible salt plug. For location see Figure 5.1.

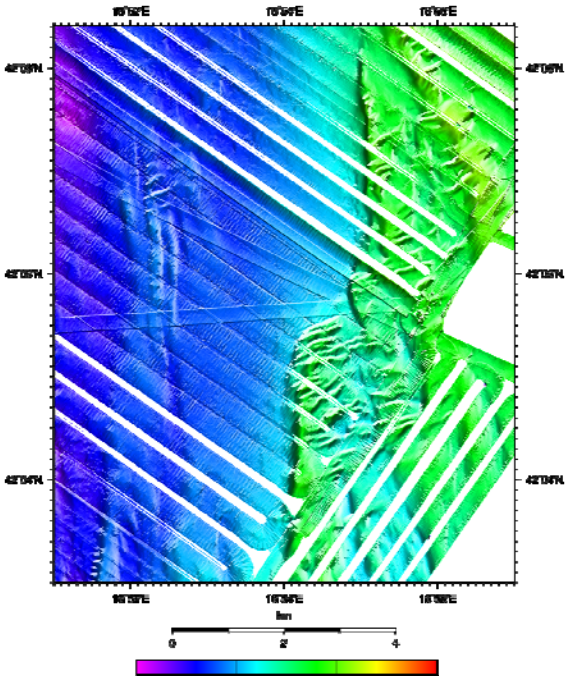

Fig. 5.4: Enlarged map of the dune field. For location see Figure 5.1.

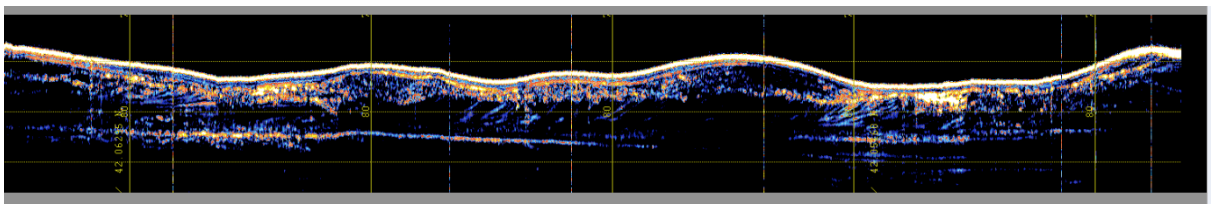

Fig. 5.5: Part of a WNW-ESE-trending PARASOUND profile (c. 6 km long) crossing the dune field. Note the foreset beds and the dominant erosion at the sea floor.

In the northwestern part of the bathymetric survey where the sea floor becomes deeper, (reaching 120 m below sea level) we imaged a thicker package of sedimentary strata (Fig. 5.6). These strata rest on top of an unconformity, often erosional, that is present throughout the surveyed area. The geometry of these strata suggests episodic fluctuation of relative sea level, with an overall transgressive trend. In the same area, we imaged a limited number of pockmark features with swath bathymetry (Fig. 5.7). They are generally less than 200 m in diameter and are roughly aligned NNW-SSE, sub-parallel to the coastal trend.

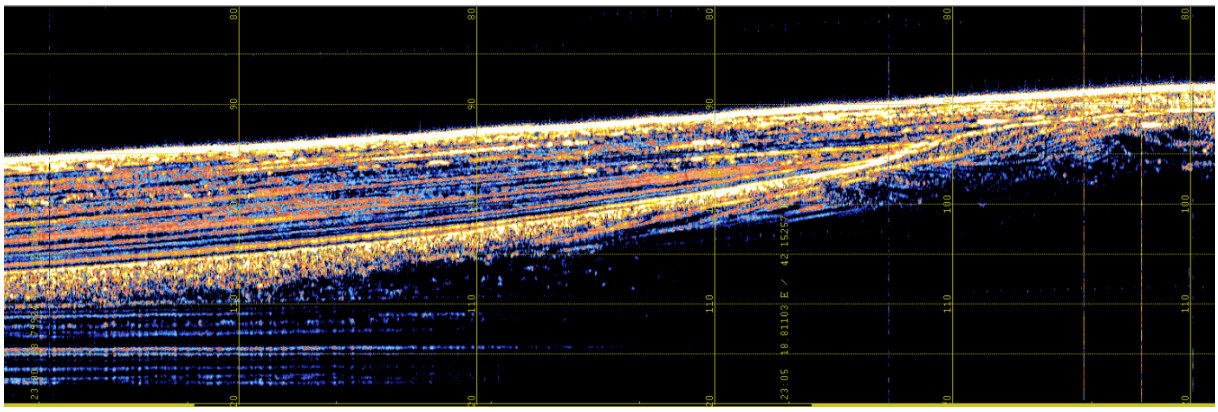

Fig. 5.6: Detail of a WNW-ESE-trending PARASOUND profile (c. 6 km long) in the deeper part of the imaged area. Note the young sedimentary unit that thickens to the NW and rests above a highly reflective unconformity. A unit with foreset beds is visible in the right-hand side, just below the unconformity.

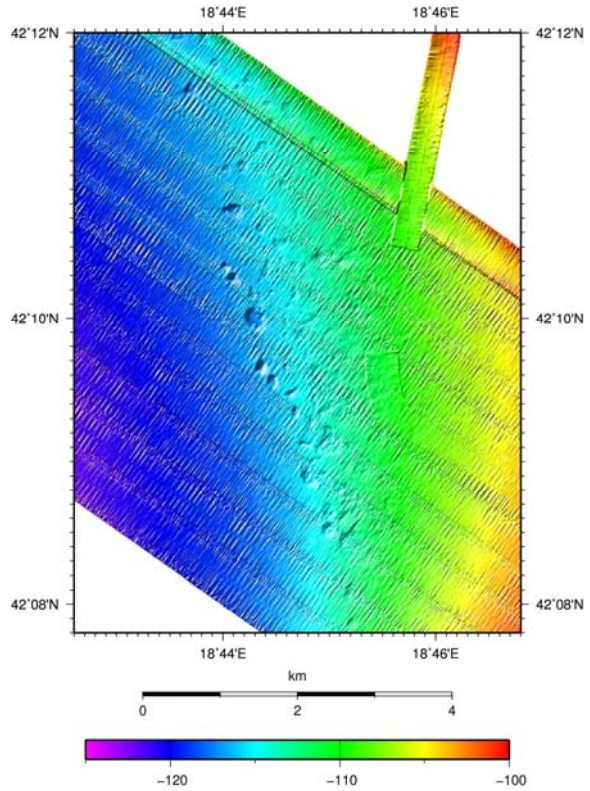

Fig. 5.7: Enlarged view of the pockmark field. For location see Figure 5.1.

5.2 Seismic Surveys

5.2.1 Seismic Instrumentation

(A. Dannowski, E. R. Flueh, H. Kopp, A. Krabbenhoeft, C. Papenberg, L. Planert, K.-P. Steffen, T. Wiskandt)

A total of 24 OBH and 12 OBS instruments from the GEOMAR pool were available for M86/3. Altogether 111 sites were deployed for refraction seismic profiling during the M86/3 cruise.

The GEOMAR OBH

The first GEOMAR Ocean Bottom Hydrophone was built in 1991 and tested at sea in January 1992. This type of instrument has proved to have a high reliability; there have been more than 5500 successful deployments since 1991.

The principle design and a photograph of the instrument during deployment are shown in Figure 5.8. The design is described in detail by Flueh and Bialas (1996).

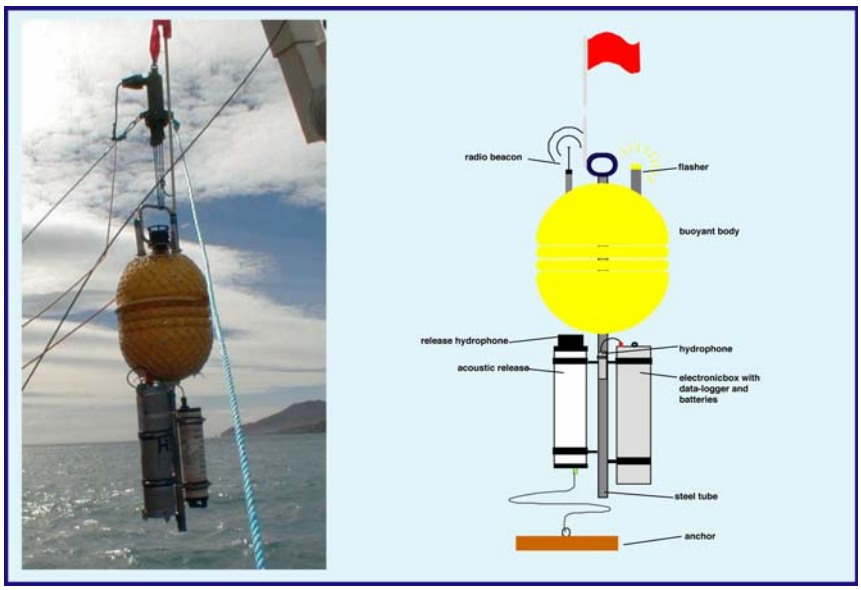

Fig. 5.8 Principle design of the GEOMAR OBH (right panel, after Flueh and Bialas, 1996) and the instrument upon deployment (left panel).

The system components are mounted on a steel tube, which holds the buoyancy body on its top. The buoyancy body is made of syntactic foam and is rated, as are all other components of the system, for a water depth of 6000 m. Attached to the buoyant body are a radio beacon, a flash light, a flag and a swimming line for retrieving from aboard the vessel. The hydrophone for the acoustic release is also mounted here. The release transponder is a model *RT661CE* or *RT861* made by *IXSea*, or alternatively a *K/MT562* made by KUM GmbH. Communication with the instrument is possible through the ship's transducer system, and ranges of 4 to 5 miles release and range commands are successful. For anchors, we use pieces of railway tracks weighing about 40 kg each. The anchors are suspended 1 to 2 m below the instrument. The sensor is a *HTI-01-PCA* hydrophone from HIGH TECH INC, and the recording device is an *MLS*

recorder of *SEND GmbH*, which is contained in its own pressure tube and mounted below the buoyant body opposite the release transponder (see Fig. 5.8).

The GEOMAR OBS-2002

The GEOMAR Ocean Bottom Seismometer 2002 (OBS-2002) is a design based on experience gained with the GEOMAR Ocean Bottom Hydrophone (OBH; Flueh and Bialas 1996) and the GEOMAR Ocean Bottom Seismometer (OBS, Flueh and Bialas, 1999). The basic system is constructed to carry a hydrophone and a small seismometer for higher frequency active-seismic profiling. However, due to the modular design of the front end it can be adapted to different seismometers and hydrophones or pressure sensors. The sensitive seismometer is deployed between the anchor and the OBS frame (Fig. 5.9), which allows good coupling with the sea floor. The three-component seismometer (KUM), usually used for active seismic profiling, is housed in a titanium tube, modified from a package built by Tim Owen (Cambridge) earlier. Geophones of 4.5 Hz natural frequency were used during M86/3. While deployed to the sea floor the entire system rests horizontally on the anchor frame. After releasing its anchor weight the instrument turns 90° into the vertical and ascends to the surface with the floatation on top. This ensures a maximally reduced system height and water current sensibility at the ground (during measurement). On the other hand the sensors are well protected against damage during recovery and the transponder is kept under water, allowing permanent ranging, while the instrument floats to the surface.

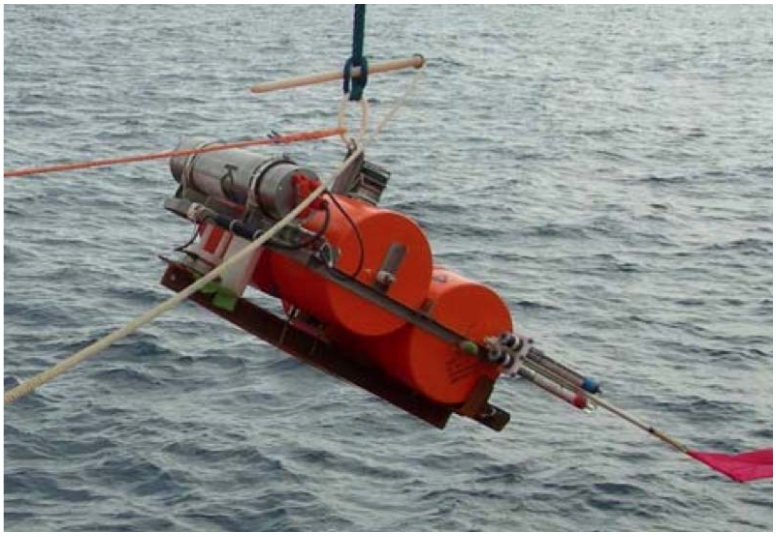

Fig. 5.9: GEOMAR OBS (Design 2002).

Seismic sources and digital streamer

During cruise M86/3 multichannel seismic data were acquired simultaneously with wide-angle refraction data acquisition. The source was a 84-liter G-Gun array. Reflection data were recorded on a GEOEEL digital streamer. Figure 5.10 provides an overview of the system setup during R/V METEOR Cruise 86/3.

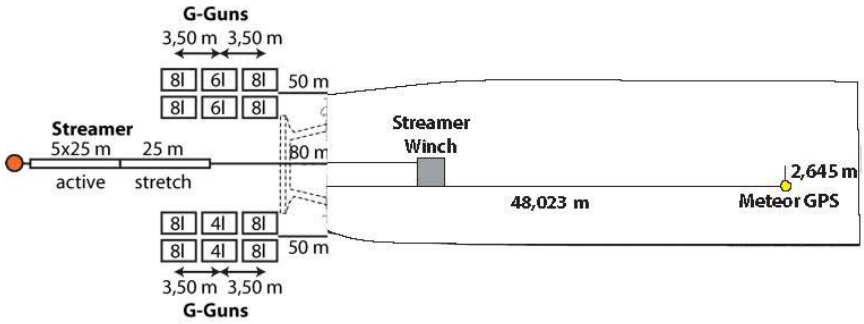

Fig. 5.10: Deck and seismic gun and streamer setting during Cruise M86/3.

G-Gun Array

The source used during surveying was a G-Gun array manufactured by Sercel Marine Sources Division (former SODERA) and Seismograph Services Inc. and consisted of 2 sub-arrays (Fig. 5.10). Six guns were set up in 3 clusters. Each cluster comprises G-Guns of 4x8 liters and in the middle either 2x6 liters or 2x4 liters (see figure). The cluster arrangement provides a good primary-to-bubble signal ratio. Operating all twelve guns simultaneously provides a total volume of 84 liters (5440cu.in.). New airgun-deployment rails mounted on R/V METEOR prior to the cruise were used to deploy G-Gun sub-arrays on aft port and starboard sides of the ship. These rails were used for the first time on R/V METEOR and they soon proved to be a major asset for handling the heavy gear during deployment and recovery operations. The arrays were towed 50 meters behind the ship's stern and 8 meters below the sea-surface. All guns were shot at ~190 bar. Shooting interval was 60 seconds for all profiles resulting in a shot point distance of 150 meters at 5 knots. The guns worked very reliably during the entire cruise.

Trigger unit

To trigger the G-guns a time-signal was generated, and fed into the Longshot trigger box. In addition, the trigger pulses were stored on a MBS recorder and displayed in real time to obtain shot times. The Clock Time Break (CTB) of the Longshot device is a TTL pulse that is 5 ms wide and represents the aim-point or the time when the guns are fired. This aim-point was set to be 60 ms after the trigger pulse. All guns were operated in auto mode; thus, guns are automatically tuned to aiming point. Exact position calculation for each shot is done by later post-processing using shot times (stored in UTC time on the MBS recorder) and GPS coordinates from the ship’s data base.

Streamer-systems

A digital streamer (GEOMETRICS GEOEEL) was used for receiving the seismic signals. The system consists of a tow cable (80 m, 24 m in the water), one stretch section (25 m) and 5 active sections (each 25 m). An active section contains 8 channels. The channel spacing is 3.25m. One AD digitizer module belongs to each active section. These AD digitizer modules are small Linux computers. Communication between the AD digitizer modules and the recording system in the lab is via TCP/IP. A failure of these A/D modules resulted in a shortening of the active streamer to a total length of only 25 meters (8 channels). A repeater was located between the deck cable

and the tow cable (Lead-In). The SPSU manages the power supply and communication between the recording system and the AD digitizer modules. The recording system is described below. Two birds were attached to the streamer. Designated streamer depth was 4 m. A small buoy was attached to the tail swivel. Shortening the active streamer length to only 8 channels (25m) did not dramatically affect the signal quality and data was recorded with good s/n ratio.

Bird Controller

Two OYO GEOSPACE Bird Remote Units (RUs) were deployed at the streamer. All RUs have adjustable wings. The RUs are controlled by a bird controller in the seismic lab. Controller and RUs communicate via communication coils nested within the streamer. A twisted pair wire within the deck cable connects controller and coils. Designated streamer depth was four meters. The RUs thus forced the streamer to the chosen depth by adjusting the wing angles accordingly. The birds were deployed at the beginning of a survey but no scanning of the birds was carried out during the survey because bird scans caused major problems with the acquisition system. However, the birds worked very reliable and kept the streamer at the designated depth.

Data acquisition systems

Data were recorded with acquisition software provided by GEOMETRICS. The analogue signal was digitized with 4 kHz. The data were recorded as multiplexed SEG-D. One file was generated per shot. The acquisition PC allowed online quality control by displaying shot gathers, a noise window, and the frequency spectrum of each shot. The cycle time of the shots is displayed as well. The software also allows online NMO-Correction and stacking of data for displaying stacked sections. Several logfiles list parameters such as shot time and shot position. Data were converted to SEG-Y files online.

5.2.2 Seismic Refraction and Reflection Data

(A. Argnani, A. Dannowski, J. Elger, E. R. Flueh, M. Handy, J. Karstens, H. Kopp, A. Krabbenhoeft, C. Papenberg, L. Planert, K. Ustaszewski)

The main research focus during M86/3 was on two wide-angle seismic profiles across the Adriatic Sea that were extended onshore in Apulia / Gargano Promontory (P2), and in Montenegro / northern Albania (P3). A total of 36 Ocean Bottom Hydrophones and Seismometers was deployed along each transect in addition to 30 onshore stations in the Dinarides and 5 onshore stations in Italy. Adjusting our work schedule to the weather and wind conditions, we also acquired a ~20 nm long shot profile parallel to the coast of Montenegro that was recorded in a fan geometry by the land stations. For this line, we deployed 3 additional OBSs to close the gap between the offshore and onshore transects. 36 ocean bottom stations were subsequently deployed along a NW-SE trending profile in the central Adriatic Sea. However, we had to end shooting of the profile ~12 hours before the scheduled end when weather conditions deteriorated during acquisition. Figure 5.11 displays the profile and instrument locations and table 1 provides profile coordinates.

	Shot number	Time	Latitude	Longitude	Waterdepth
P01	S1	1:37:12.0042	41° 53' 28.59'' N	17° 39' 21.33'' E	1117 m
	S1215	21:51:00.42	42° 52' 52.52'' N	15° 43' 43.78'' E	148 m
P02	S1	10:00:22.021	42° 62' 02.22'' N	18° 56' 43.48'' E	64 m
	S1547	11:46:01.021	40° 46' 23.13'' N	17° 47' 08.43'' E	81 m
P03	1	07:28:31.021	41° 51' 41.48'' N	16°17' 23.43'' E	23.3 m
	1675	11:22:16.021	42° 01' 04.17'' N	19°05' 06.19'' E	42.5 m
P04	1	08:29:06.000	42° 14' 18.14'' N	18° 46' 45.67'' E	89.3 m
	300	13:27:59.000	42° 00' 40.81'' N	19° 06' 28.94'' E	32.8 m

Table 1: Profile coordinates for refraction profiles P01-P04.

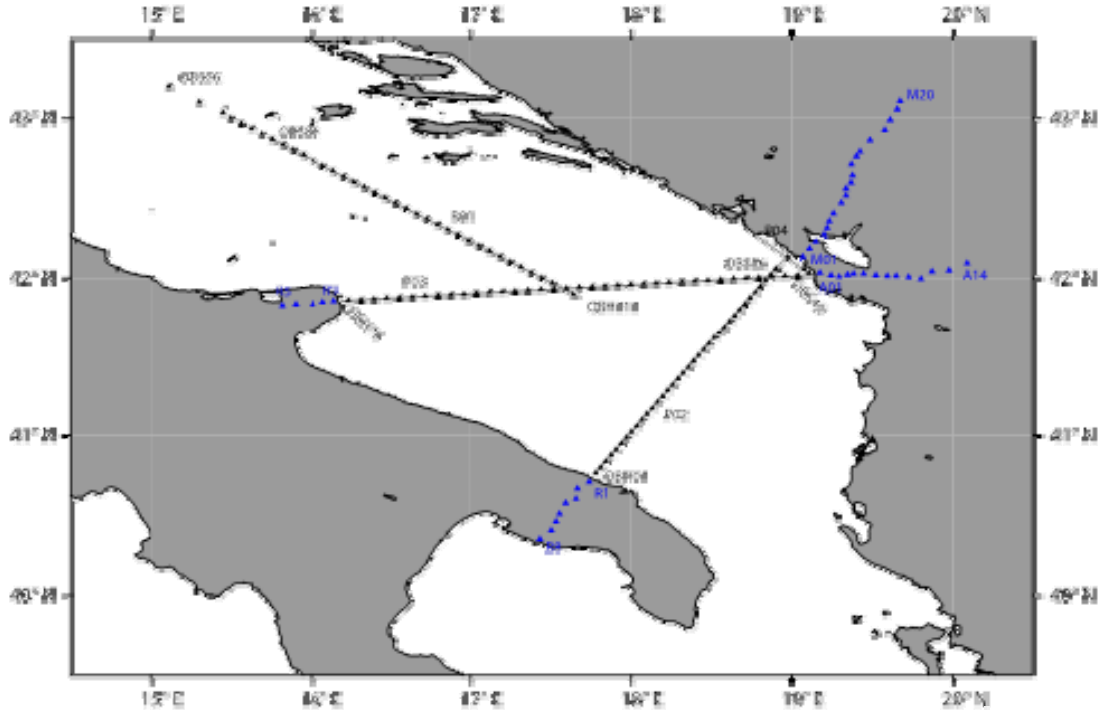

Fig. 5.11: Profile locations of seismic lines acquired during M86/3.

Wide-angle seismic Profile P01

36 instruments were deployed at 3.6 nm spacing along the 165 nm long profile P01. Shooting started in the SE and had to be terminated after passing OBS83 (Fig. 5.12) due to deteriorating weather conditions. Before that, a shot spacing of ~140 m corresponding to a ship's speed of 5 kn at an interval of 60 s was chosen to cover most of the profile.

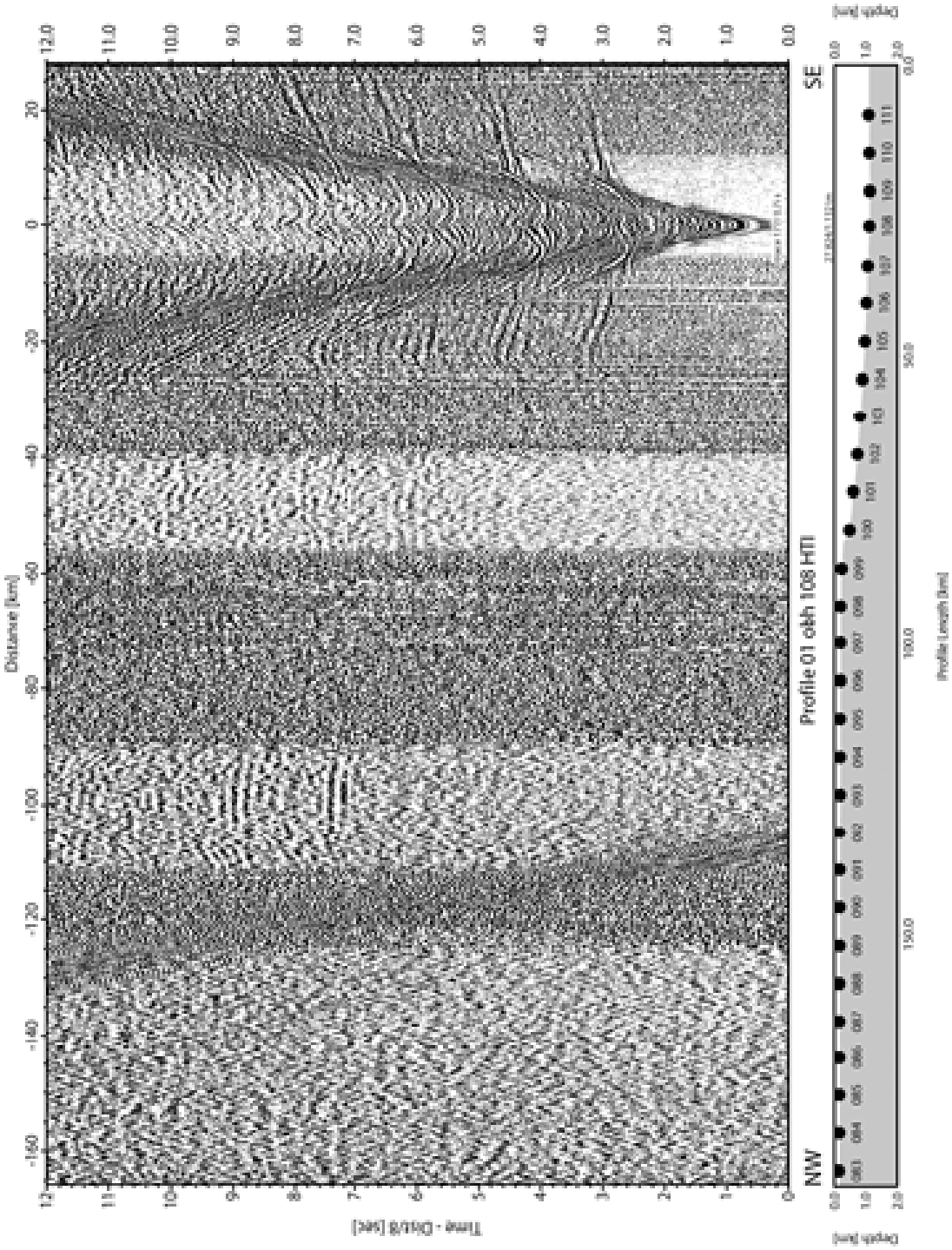

Fig 5.12: Record section of OBH 83, Profile PO1

During shooting of P01, a commercial seismic survey was carried out simultaneously, resulting in a decreased signal-to-noise ratio on our data as described below for P02. Nevertheless, the majority of stations recorded seismic arrivals with up to 120 km offset. Moho phases are recorded on a number of stations towards the SE end of the profile (OBH110, 108, 107, 104, 103, 101) as well as on reverse shots (OBH 97-93) and will yield the depth to the crust-mantle transition during subsequent modeling.

Wide-angle seismic Profile P02

36 instruments were deployed at 2.7 nm spacing along the 98 nm long profile P02, which trends from Apulia to Montenegro. A shot spacing of ~100 m was chosen (trigger interval of 60 s at a ship's speed of 4.0 kn) for shooting the 6 G-gun clusters with a combined volume of 84 l. The streamer data are described below. During shooting of P02 a commercial seismic survey was conducted in Croatian waters offshore Montenegro. Their airgun signal caused a decreased signal-to-noise ratio on our seismic sections, manifested in alternating 'stripes' (Fig. 5.13).

OBH22 is located in the northeastern portion of the foreland basin (Fig. 5.13) and exhibits refracted waves in the sedimentary layers. These show a time gap indicative of a low velocity zone. This offset is observed on numerous stations in the basin (e.g. OBS25, OBH23, OBH21 and others). A clear basement reflection / refraction following the sedimentary phases is identified on most stations located in the foreland basin (OBH14-22).

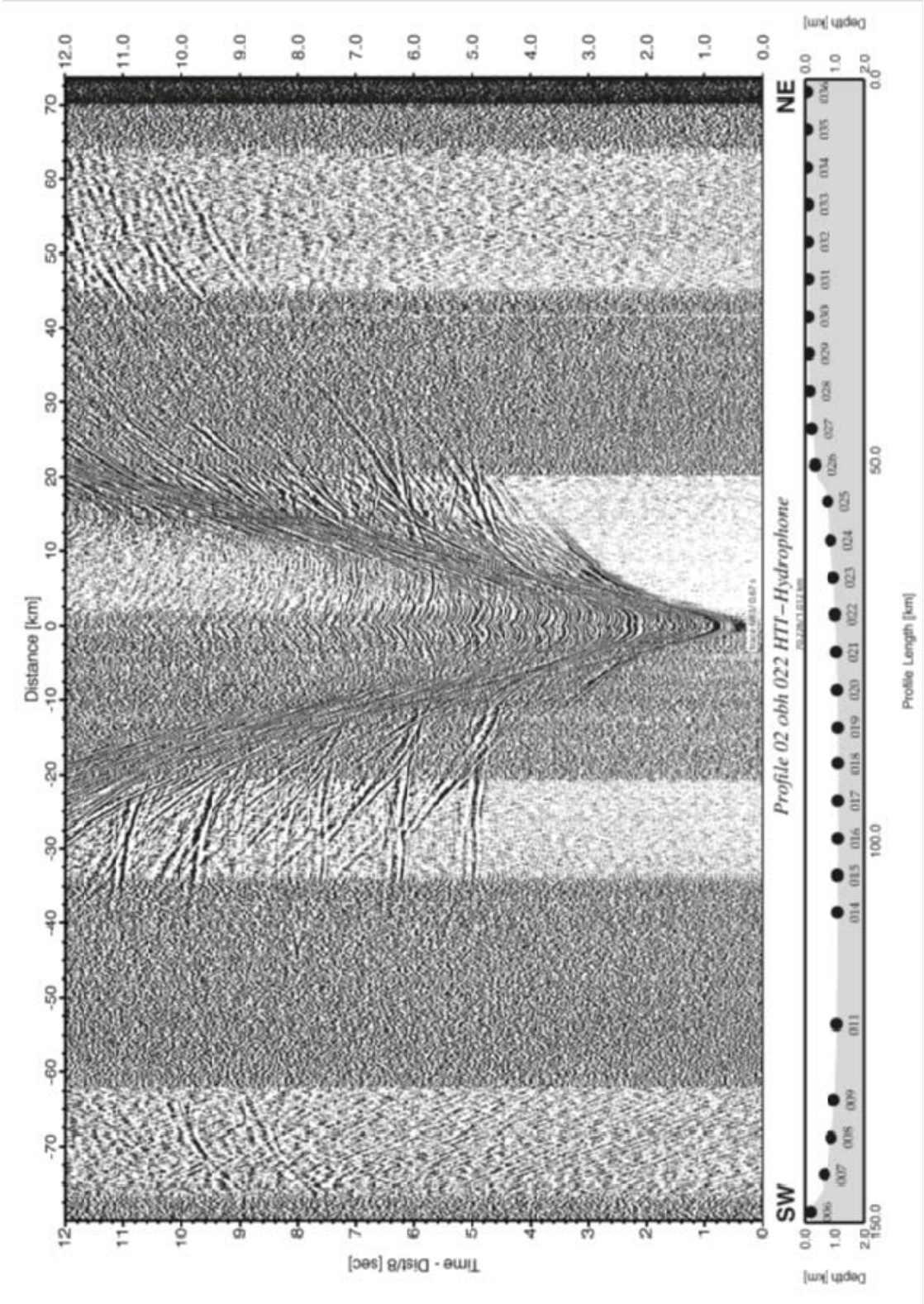

Fig. 5.13: Record section of OBH 22, Profile P02.

The water depth along P02 changes from a shallow domain on the Apulian and Adriatic-Dinaric platforms (less then 150 m) to a deeper domain (> 1100 m) in the center of the basin. This is documented by the decreasing velocities towards the basin at OBH05, where positive

offsets cover the sedimentary sequence of the basin infill and negative offsets towards the Apulian platform show higher velocities through the carbonate platform.

Hence, record sections from stations located near the platform-basin transition are affected by the variable morphology and result in high apparent velocities. This is also true for large offsets and deep phases (e.g., Moho reflection on record section of OBH22, Fig. 5.13 at offsets of 60-80 km).

On the Apulian platform, the Moho reflection is recorded on stations OBH01, OBH02, OBH05, OBH06 and OBH11 and will allow clear imaging of the crustal thickness beneath the Adriatic basin.

For initial forward modeling of P02 using the program RAYINVR of C. Zelt, we picked sedimentary and crustal phases as well as Moho reflections of selected stations along P02 (Fig. 5.14).

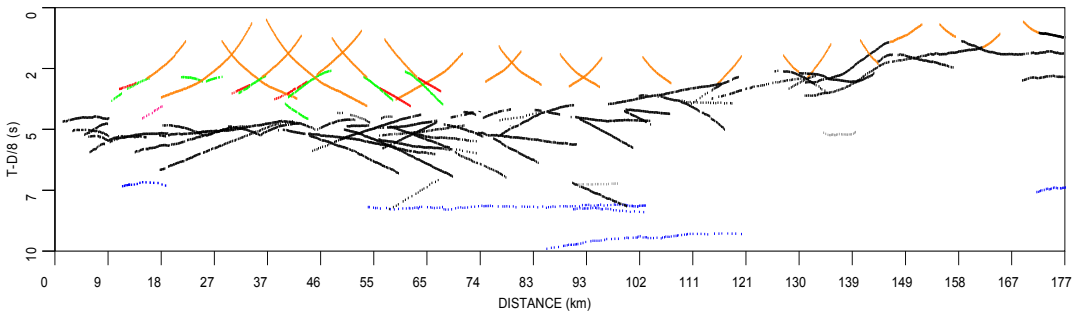

Fig. 5.14: Picking of selected sedimentary, crustal and mantle phases along P02.

Information from the streamer data was used to constrain the basement depth and geometry of the continental platform (Fig. 5.15). The central Adriatic basin is filled by 3 km of sediment on average. A low velocity zone is underlain by the basement, where velocities increase from ~5 km/s to 7.2 km/s at the Moho. A deepening of the Moho reflector by 8 km from Italy towards Montenegro is required to fit the recorded mantle phases.

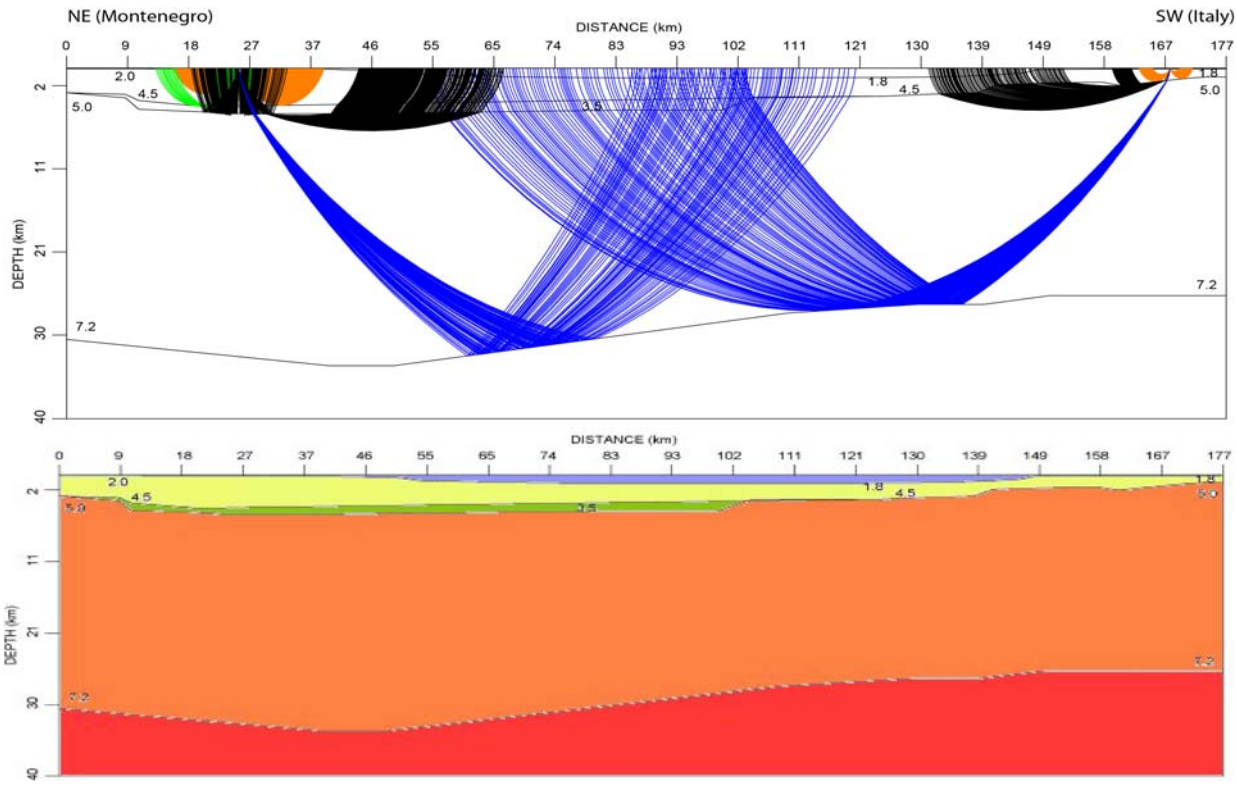

Fig. 5.15: Selected ray path (upper panel) and preliminary forward model (lower panel) along P02. Note that Montenegro coast (NE) is to the left and Italian coast (SW) is to the right; compare Fig. 5.17.

Wide-angle seismic Profile P03

P03 trends approximately E-W from the Gargano Promontory in Italy to northern Albania. The 36 ocean bottom stations along this 130 nm long line are spaced at 3.6 nm. A shot interval of 60s at the ship's speed of 4.5 kn resulted in an approximate shot spacing of ~140 m. All 6 G-gun clusters were in operation during shooting. The corresponding streamer data are discussed below.

Also along this profile a clear Moho reflection was recorded at many stations (OBH55, OBH58-59, OBH61, OBH64-65, OBH67, OBH69-72, OBH74) and will facilitate a detailed analysis of the crustal thickness and location of the crust-mantle boundary beneath the foreland basin. Stations located on the basin floor recorded the refracted waves through the sedimentary succession as well as a reflection from the basement and refracted arrivals from the crust.

The record of OBS45 on the Adriatic platform (Fig. 5.16) shows arrivals from the sedimentary cover, as well as a basement reflection and refracted waves through the crust. A clear Moho reflection is identified at offsets ranging from -60 to -100 km.

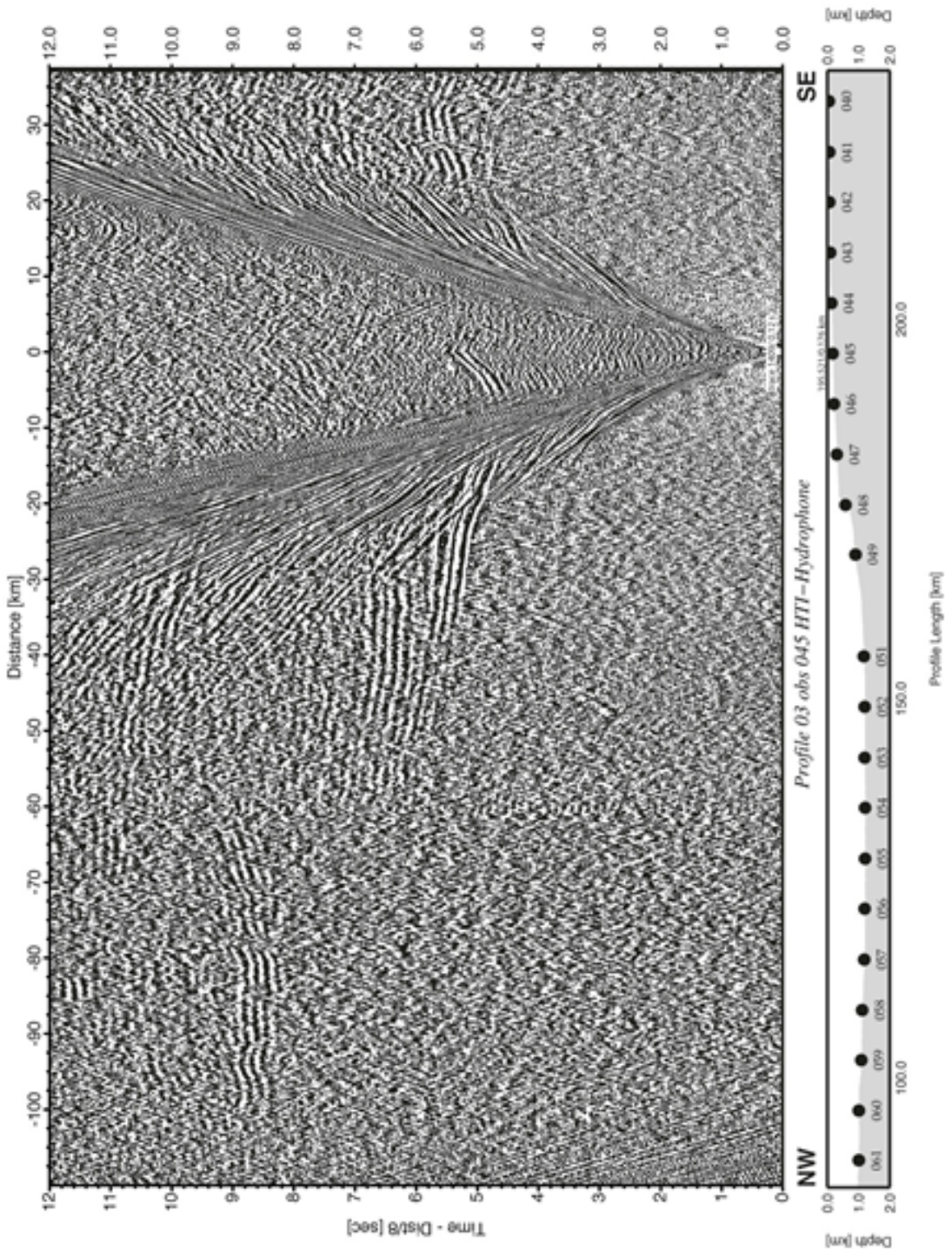

Fig. 5.16: Record section of OBH 45, Profile P03.

Multichannel Seismic Reflection Data

Reflection seismic data were acquired with the 8-channel streamer while shooting the refraction profiles. The large energy (volume of 84 l) used in acquiring refraction data limited the resolution of the reflection data and the processing improvement. Nevertheless, the quality of the reflection seismic data is good enough to grasp the main features in this area; in particular, profiles P02 (Fig. 5.17) and P03 (Fig. 5.18) offer a remarkable image of the whole southern Adriatic basin, from coast to coast.

Profiles P02 and P03 converge on the same part of offshore Montenegro and therefore show similar features, but the two profiles transect very different areas on the Italian side of the Adriatic: profile P02 crosses the Apulian platform, a stable part of the Adriatic microplate made up of undeformed foreland of both the Apennines and Hellenides. In contrast, the W end of profile P03 is at tip of the Gargano Promontory, which comprises deformed foreland of the Apennine orogen (Argnani et al. 2009 and refs. therein). For this reason, the description below of the Montenegro side of the platform uses both P02 and P03, whereas the two profiles are described separately at the Italian end.

The margin of the Apulian platform

The Apulian region (Puglia) represents the undeformed part of the African foreland which is deflected downwards at both ends under the load of the encroaching nappe stacks of the Apenninic (NW) and Dinaric-Hellenic (SE) Orogens. Apulia is located in the bulge of the upwardly flexed African lithosphere (Moretti and Royden, 1988) and is characterized by a flat plateau that exposes Cretaceous shallow water carbonates. Exploration wells and commercial seismic data indicate that these Mesozoic platform carbonates are several km thick, and pass eastwards through a steep margin to a thinner, time-equivalent succession composed of pelagic limestones (De Dominiciis and Mazzoldi, 1987; Argnani et al., 1993; Nicolai and Gambini, 2007).

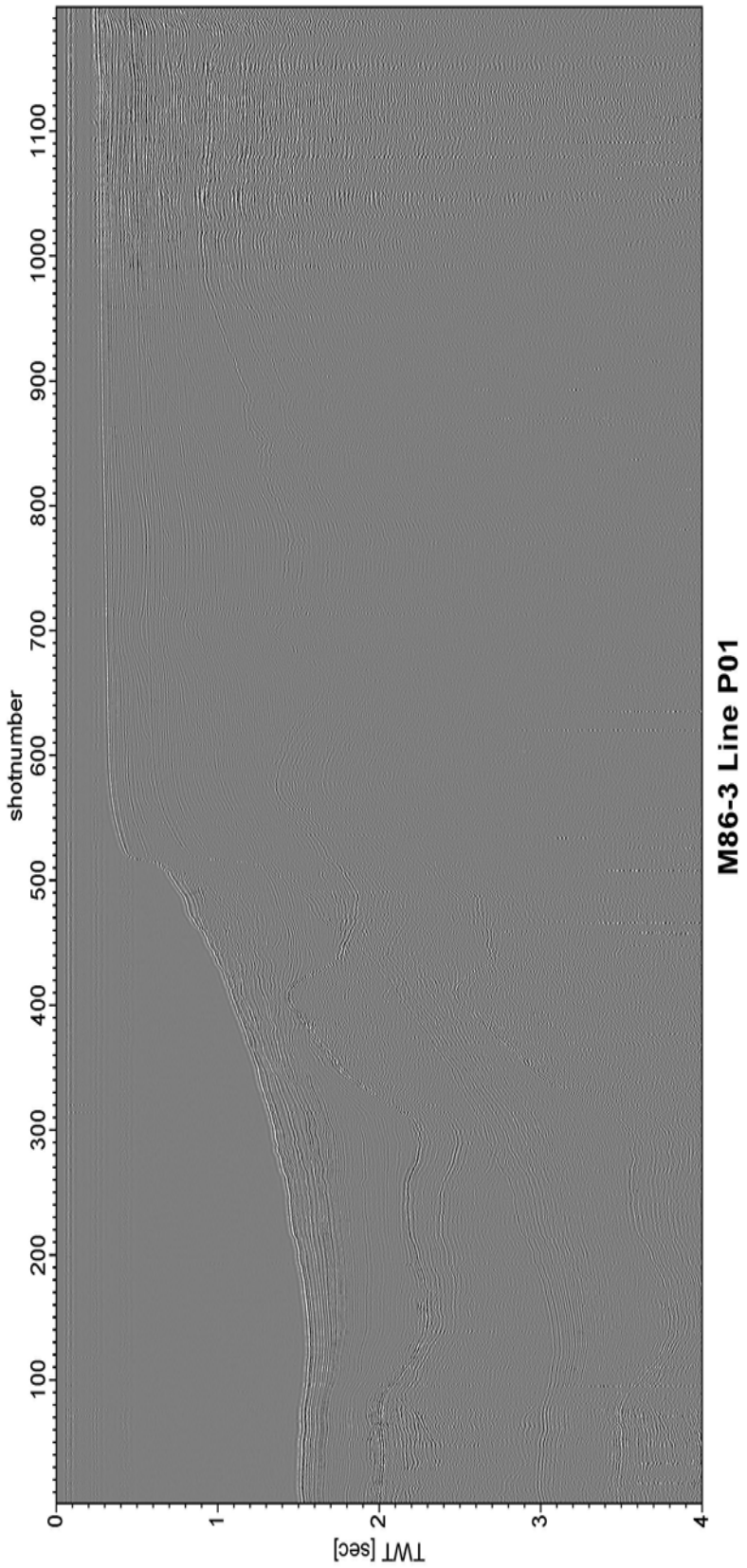

Fig. 5.17: Profile P01 along the southern Adriatic. Uninterpreted seismic section showing structure of the Ionian Basin with Late Miocene (including Messinian) to Plio-Pleistocene sediments.

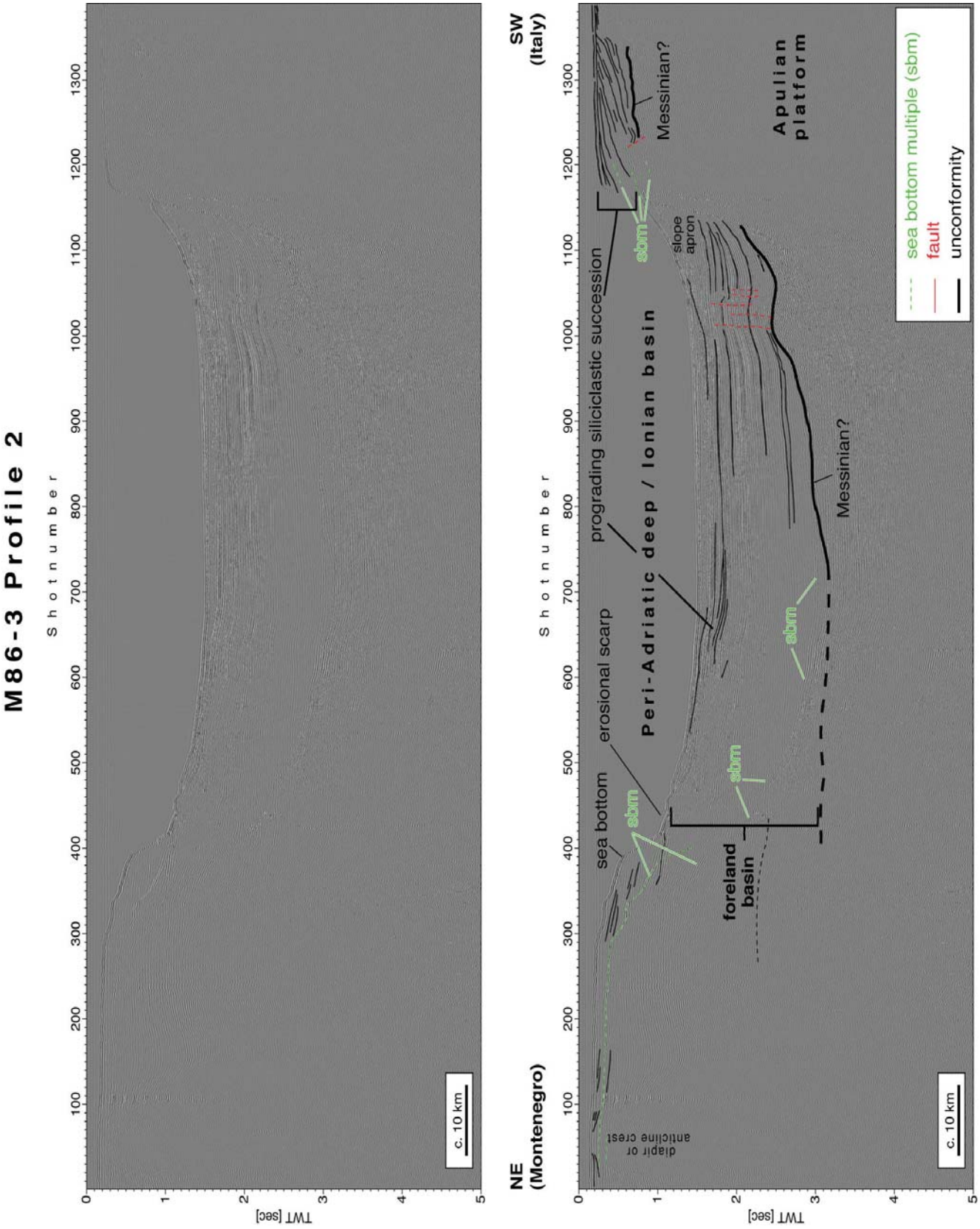

Fig. 5.18 Profile P02 across the southern Adriatic from Bar (Montenegro) to north of Brindisi (Italy). Uninterpreted section (above) and interpreted section (below) showing structure at the two ends of the Apulian platform, separated by Late Miocene (including Messinian) to Plio-Pleistocene sediments of the Ionian Basin.

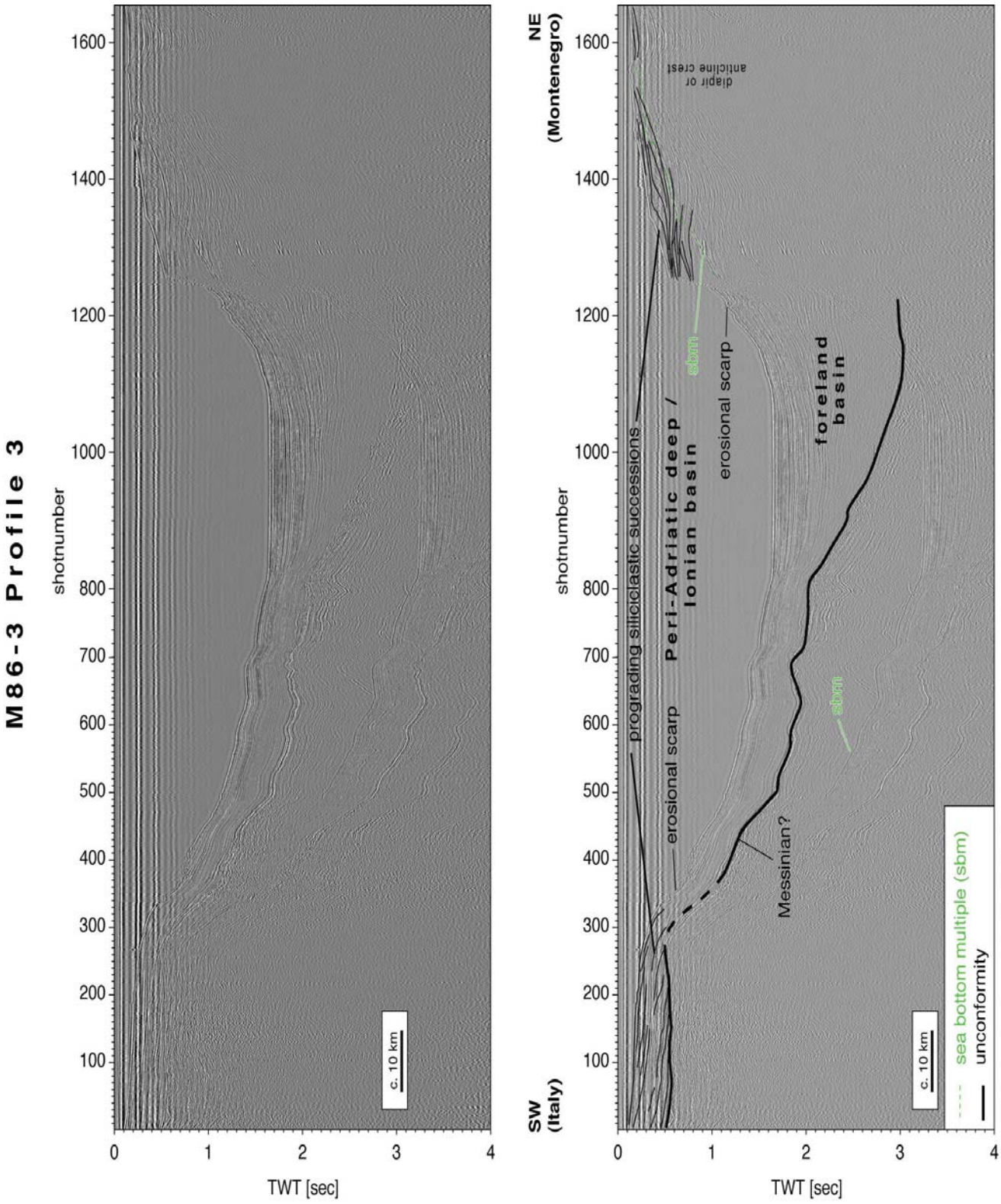

Fig. 5.19: Profile P03 across the southern Adriatic Sea from Bar (Montenegro) to the Gargano Promontory (Italy). Uninterpreted section (above) and interpreted section (below) showing prograding fans at both ends. The thicker one in the NW is associated with the Apenninic accretionary wedge, located just to the NW.

The Mesozoic Apulian carbonate platform and its steep margin appear clearly on the Italian side of profile P02 (Fig. 5.18); our images are comparable with the geometry observed in a commercial seismic profile (Fig. 5.20). The top of the platform occurs at a depth corresponding to a TWT of about 700-800 ms. A prograding unit of Plio-Pleistocene clastic sediments corresponding in thickness to a TWT of 500 ms rests unconformably above the platform carbonates. Exploration wells indicate that the Mesozoic units deepen considerably to the east of the Apulia platform. Although the resolution of our reflection seismic profiles is not sufficient to image the top of the pelagic carbonate units, a unit of clastic sediments with thickness corresponding to a TWT of 2 to 3s is visible in the southern Adriatic basin. The strata of this unit are sub-horizontal to slightly E-dipping and rest unconformably on an eastward-dipping unconformity. The unconformity shows evidence of erosion towards the margin of the Apulian platform and can be interpreted as having been produced during the Messinian sea-level drop; therefore, the overlying sediments are Plio-Quaternary age. Although masked by the multiples, the Plio-Quaternary sedimentary unit continues to thicken eastward.

Offshore Gargano Promontory

The Gargano Promontory protrudes into the Adriatic Sea with a remarkable elevation (locally > 1000 m) and coincides with a broad (ca. 25 km wide), E-W trending anticline. Cretaceous (Maiolica) limestones of the Apulian platform are exposed on the western side of the promontory, whereas Mesozoic slope and basinal limestones crop out on the eastern side. Open folds in Neogene (Mio-Pliocene) sediments are subtle indications of diffuse intraplate deformation (e.g., Argnani et al., 2009 and ref. therein). This may be related to limited seismicity in the vicinity of the Gargano Promontory that includes mostly deep-seated compressional earthquakes with NNW-trending P axes (Vannucci et al., 2004).

Figure 5.20 shows reflectors interpreted to be Plio-Quaternary sediments with a progradational geometry (possibly applies only to Quaternary sediments) and resting unconformably on the previously folded Mesozoic and Cenozoic rocks. This unconformity merges towards the basin with an unconformity at the base of the Plio-Quaternary sediments, and that we interpret to be the Messinian unconformity. Towards the basin centre, where the bottom multiples are deeper, some strata are imaged below the unconformity. Some minor folding and faulting affect the Plio-Quaternary sedimentary succession along the basin slope, although this deformation seems to die out in the uppermost sedimentary strata. The Messinian unconformity can be followed all the way to the Montenegro shelf where it attains a depth corresponding to a TWT of 3s.

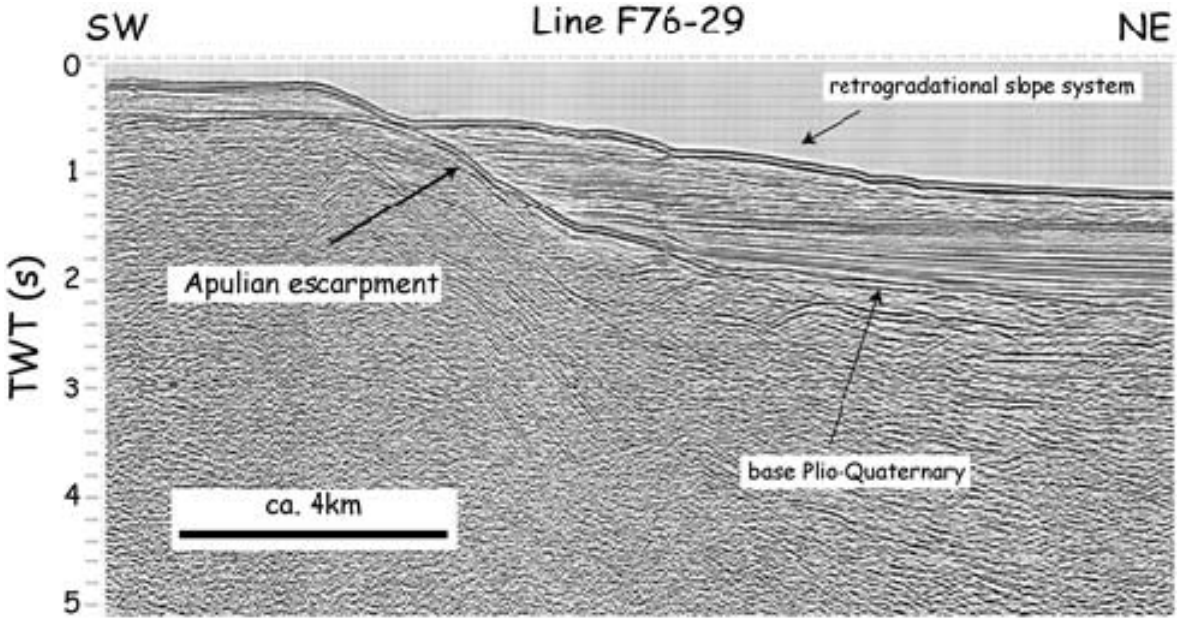

Fig. 5.20: Commercial seismic profile of offshore Brindisi showing the steep margin of the Apulian platform (modified from VIDEPI http://unmig.sviluppoeconomico.gov.it).

Offshore Montenegro

The Plio-Quaternary foredeep sedimentary fill toward the coast of Montenegro (Figs. 5.18-5.19) has a thickness corresponding to a TWT of c. 3s. A broad shelf c. 30 km wide on the Montenegro side of the Adriatic Basin has a stack of several progradational units at its edge (Fig. 5.19), with the foreset strata truncated on the slope of the basin. Towards the coast of Montenegro, the reflection pattern shows a 7-8 km wide anticlinal feature. Although partly masked by multiples, the tilt of the flanking strata increases downward, as far as a depth equivalent to 2s TWT. The axial plane of the anticline dips steeply towards the west, as also observed in a commercial profile from the same area (Fig. 5.20). The seismic images and the data above obtained from swath bathymetry and sub-bottom profiling suggest that the anticlinal shape may be an evaporite diapir, although interaction with thrusting of the Dinarides, which is very close, cannot be ruled out. The interaction between thrusts and evaporites is rather common in the deformed Ionian succession exposed in southern Albania (e..g., Velaj et al., 2000), and data supporting the occurrence of a salt wall along the Montenegro thrust front are available in unpublished reports (Fig. 5.21, Glavatovic, Seismotectonics report, undated) .

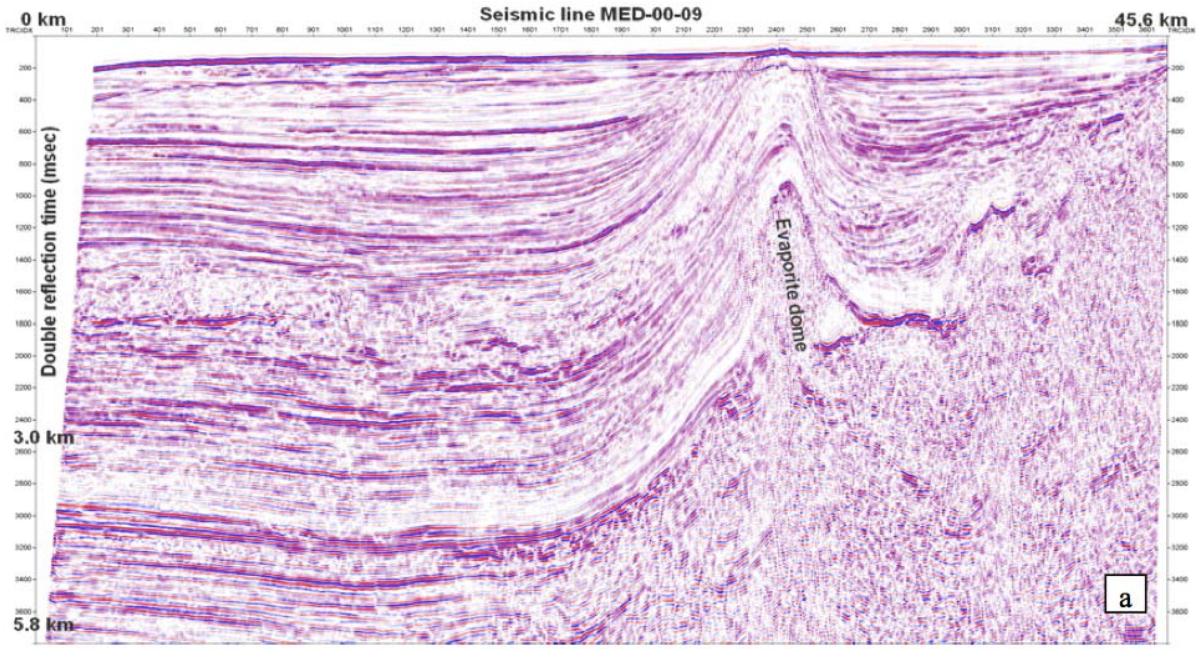

Fig. 5.21: Commercial seismic profile of offshore Montenegro from report of Glavatović. The profile trends SW (left) to NE (right) and is located near the eastern ends of our P02 and P03 sections. The "evaporite dome" is the same feature imaged in our multichannel reflection profiles and shows a steep dip to the SW, as also observed in P03.

Evidence for repeated slope instability

The reflectors of the uppermost prograding units on either side of the southern Adriatic Basin show evidence of gravitational instability. On the Montenegro side, a stack of prograding units is clearly imaged at the shelf edge and the strata are sharply truncated along the basin slope (Fig. 5.19). Similarly truncated prograding strata are observed on the Apulian side (Fig. 5.18), for example, where a slide scar some 50m long that dissects the uppermost sediments is imaged offshore of Gargano (Fig. 5.19). Taken together, these structures suggest that the sediments deposited on the upper slope were (repeatedly?) affected by slumping/sliding. In fact, swath bathymetry surveys indicate that slides and slumps of various sizes extensively affected the eastern margin of the southern Adriatic Basin (Argnani et al. 2011).

Additional evidence for widespread mass wasting comes from the central part of the basin (Fig. 5.18) which is covered by large units with transparent to chaotic seismic structures and a thickness corresponding to a TWT of about 200 ms. This may represent a mass-transport deposit from one of more very large events, for example, slope failures that affected the adjacent basin margins.

Amphibious transects: On-shore stations

In continuation of profiles P02 and P03, seismic stations were deployed on land in Albania, Montenegro and Italy (Fig. 5.11). Five seismic stations were deployed extending profile P03 to the west. On the Albanian side of this profile 14 stations were installed with a similar spacing of 6 km. Profile P02 was extended by 20 stations deployed in Montenegro on the Northern end of the line reaching 130 km into the land, thus recording to an offset of 300 km. On the Southern end of this profile in the Apulia region, 8 stations recorded the shots of P02. They were installed at an average spacing of 6 km with an offset of 3 km from the coast.

All record sections show usable seismic phases, with variable quality depending on the distance from the coastline and local site conditions (e.g. Fig. 5.22-5.23). Only the central stations in Montenegro and Albania show a lower signal-to-noise ratio.

In general, first arrivals with apparent velocities ranging from 5.5 km/s to 7 km/s are evident up to 50 km offset. At larger offsets, data show an evident decrease in signal-to-noise ratio. On both sides of the Adriatic sea, the data show shadow zones. The data quality is satisfactory but first arrivals are barely visible and coherent arrivals with similar velocities appear abruptly at later times. Those time gaps are indicative of low velocity regions. The crustal phases are visible up to 110 km offset and tend to large amplitude PmP reflections, which exhibit excellent lateral coherence and continuity (compare to Fig. 5.22). At larger offsets mantle refractions have been observed up to offsets of 240 km.

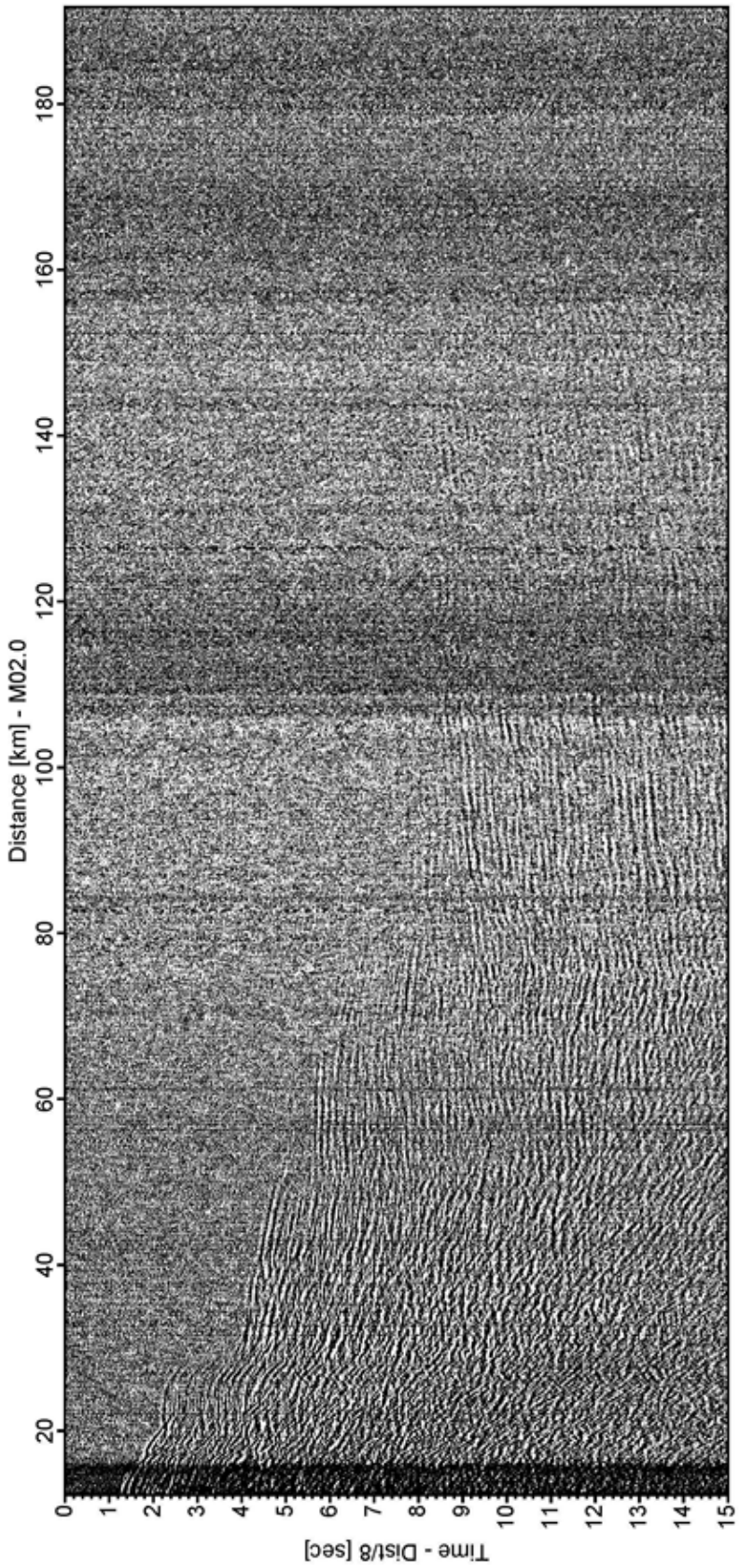

Fig. 5.22: M02 Montenegro landstation, 15 km to shore.

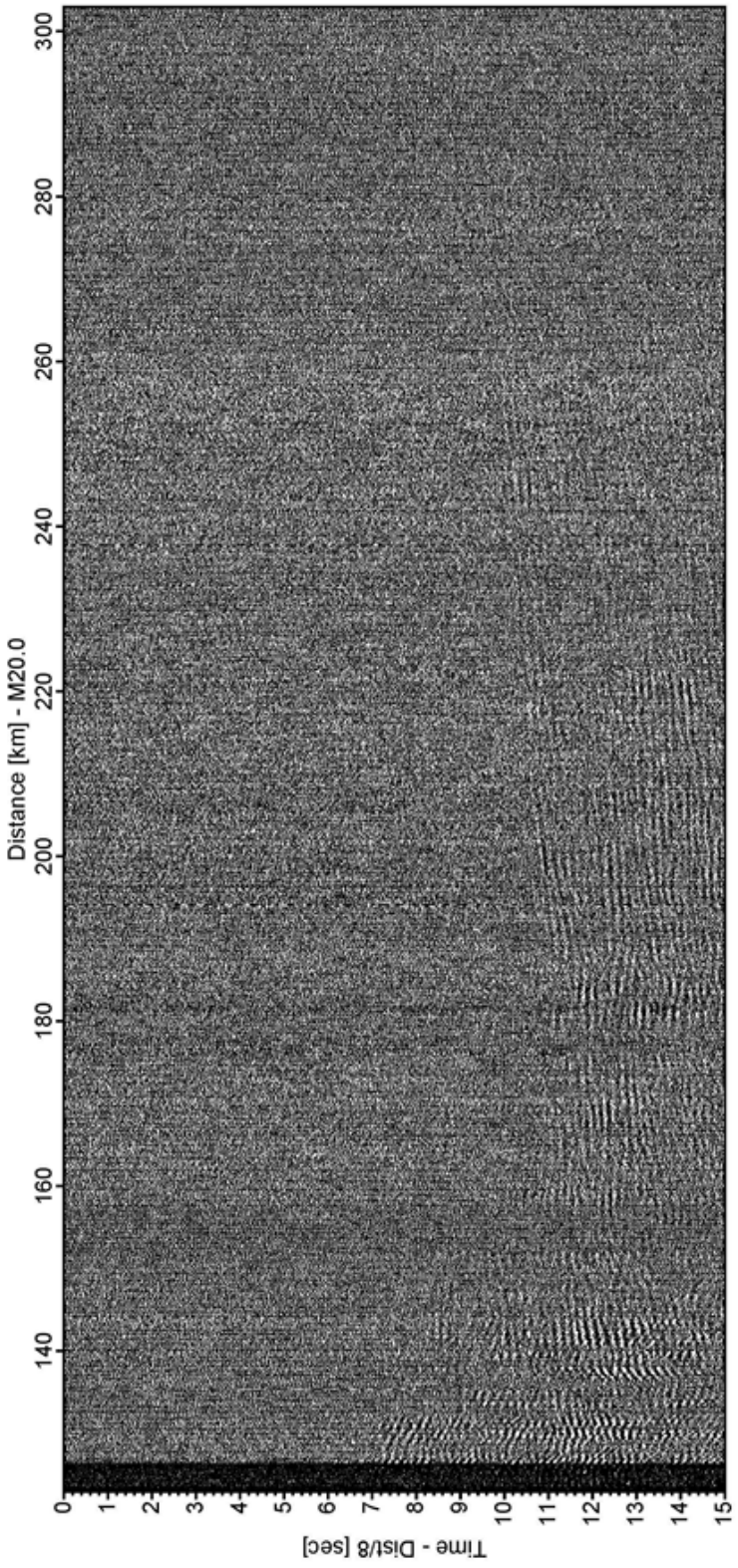

Fig 5.23: M20 Montenegro landstation, 130km to shore.

6 Ship's Meteorological Station

(B. Frey)

The research vessel Meteor left port of Brindisi on January, 20th at 9 o'clock. The first project could be performed until January 23rd, in calm seas and at little cloud cover. Because of the forecasted heavy squalls and waves of up to 4m for the 25th, the original plan was extended to drive an additional bathymetric measurement series in the calmer waters off the Montenegrin coast. During that time raged a storm at average wind speeds of 9Bft and some hurricane-force gusts on the original planned route. Up to 26th the wind calmed down so the interrupted program could picked up again and this section could be completed successfully.

The longest test section on this trip had to be shortened because of some forecasted heavy storms. Expected wave heights of over 4m and katabatic winds (Bora) in hurricane strength made this necessary at the night of 31st to February 1st . Even under the protection of land at the island of Vis, numerous gusts of 11Bft occurred. A gust of 12Bft was recorded on the 1st of February at 13:39 UTC. However, the sea kept a moderate hight at 1-1.5m, while at the same time the open sea showed wave heights of more than 5 meters.

On the morning of February 2nd we were able to resume sailing and start hauling the hydrophones and seismometers at 2-3m waves and winds of 7 Bft. On the night from 2nd to 3rd we could still register some gusts of 9Bft. This coincided with the prediction which announced stronger winds and higher waves for the southern end of this measurement section. For that reason the collecting of the measurement equipment had to be done quickly. The last hydrophone was taken on board on February 3rd at 7:30 UTC and we set course to Dubrovnik.

Because of expected hurricane-force gusts and wave heights of 4m, an additional planned route for some bathymetric measurements were not performed. Instead, we ended the trip M86 / 3 on February 3rd, 19:00 UTC at the port of Dubrovnik.

7 List of Stations

Station	Instrument	date	time	lat	lon	depth	Recorder	Hyd	Geophone
ME863/193-1	OBS76	30.01.12	03:53	43°12.097' N	15°06.210' E	200 m	991258	OAS 14	Owen 0708-099
ME863/194-1	OBS77	30.01.12	04:56	43°06.081' N	15°18.018' E	204 m	061201	OAS 51	Owen 1001-114
ME863/195-1	OBS78	30.01.12	05:40	43°02.081' N	15°26.810' E	176 m	991242	HTI 108	Owen 0509-075
ME863/196-1	OBS79	30.01.12	06:08	43°00.084' N	15°29.695' E	161 m	991248	OAS HH	Owen 1001-115
ME863/197-1	OBS80	30.01.12	06:35	42°58.076' N	15°33.625' E	152 m	991255	HTI 44	Owen 1001-118
ME863/198-1	OBS81	30.01.12	07:03	42°56.068' N	15°37.494' E	149 m	010401	HTI 97	Owen 1001-116
ME863/199-1	OBS82	30.01.12	07:32	42°54.123' N	15°41.426' E	148 m	000712	OAS 34	Owen 0104-002
ME863/200-1	OBS83	30.01.12	08:03	42°52.122' N	15°45.393' E	149 m	040807	OAS 87	Owen 1001-120
ME863/201-1	OBS84	30.01.12	08:33	42°50.054' N	15°49.217' E	155 m	110101	HTI 38	Owen 34
ME863/202-1	OBS85	30.01.12	09:04	42°48.060' N	15°53.140' E	159 m	061202	HTI 61	Owen 1001-121
ME863/203-1	OBS86	30.01.12	10:13	42°46.064' N	15°56.988' E	162 m	991250	HTI 27	Owen 0509-073
ME863/204-1	OBS87	30.01.12	10:40	42°44.091' N	15°00.873' E	165 m	Sercel	HTI 42	Owen 1001-113
ME863/205-1	OBH88	30.01.12	11:13	42°42.094' N	16°04.785' E	165 m	020503	HTI 116	
ME863/206-1	OBH89	30.01.12	11:47	42°40.079' N	16°08.708' E	167 m	001001	HTI 40	
ME863/207-1	OBH90	30.01.12	12:15	42°38.064' N	16°12.578' E	170 m	040803	OAS 35	
ME863/208-1	OBH91	30.01.12	12:44	42°36.039' N	16°16.501' E	174 m	991251	OAS 21	
ME863/209-1	OBH92	30.01.12	13:13	42°34.058' N	16°20.363' E	178 m	040602	HTI 118	
ME863/210-1	OBH93	30.01.12	13:42	42°32.050' N	16°24.301' E	342 m	010403	HTI 49	
ME863/211-1	OBH94	30.01.12	14:11	42°30.033' N	16°28.198' E	187 m	010402	HTI 64	
ME863/212-1	OBH95	30.01.12	14:40	42°28.043' N	16°32.067' E	189 m	010406	HTI 93	
ME863/213-1	OBH96	30.01.12	15:10	42°26.027' N	16°35.982' E	195 m	991256	HTI 53	
ME863/214-1	OBH97	30.01.12	15:37	42°24.005' N	16°39.904' E	199 m	991240	HTI 109	
ME863/215-1	OBH98	30.01.12	16:05	42°22.010' N	16°43.789' E	205 m	991260	HTI 78	
ME863/216-1	OBH99	30.01.12	16:30	42°20.002' N	16°47.682' E	235 m	050810	HTI 68	
ME863/217-1	OBH100	30.01.12	16:58	42°18.007'N	16°51.575'E	485 m	081201	OAS45	
ME863/218-1	OBH101	30.01.12	17:25	42°16,007'N	16°55.497'E	607 m	090702	OAS 96	
ME863/219-1	OBH102	30.01.12	17:54	42°13.995'N	16°59.354'E	747 m	041101	HTI 120	
ME863/220-1	OBH103	30.01.12	18:20	42°12.028'N	17°03.275'E	832 m	040101	HTI 23	
ME863/221-1	OBH104	30.01.12	18:47	42°10.007'N	17°07.171'E	912 m	010409	HTI 102	
ME863/222-1	OBH105	30.01.12	19:17	42°7.990'N	17°11.083'E	984 m	040102	HTI 81	
ME863/223-1	OBH106	30.01.12	19:48	42°05.985'N	17°14.943'E	1039 m	061204	HTI 119	
ME863/224-1	OBH107	30.01.12	20:18	42°03.967'N	17°18.874'E	1074 m	991249	HTI 110	
ME863/225-1	OBH108	30.01.12	20:50	42°01.992'N	17°22.789'E	1124 m	991247	HTI 115	
ME863/226-1	OBH109	30.01.12	21:22	42°0.000'N	17°26.654'E	1142 m	050811	HTI 114	
ME863/227-1	OBH110	30.01.12	21:55	41°58.000'N	17°30.504'E	1126 m	010404	OAS 15	
ME863/228-1	OBH111	30.01.12	22:27	41°55,995´N	17°34,442É	1106 m	991243	OAS 12	

Station	Instrument	deployment					Recorder	Hyd	Geophone
		date	time	lat	lon	depth			
ME863/035-1	OBH01	20.01.12	14:51	40°48.147' N	17°48.658' E	90.7 m	040803	HTI 116	-
ME863/036-1	OBH02	20.01.12	15:24	40°50.341' N	17°50.556' E	101.5 m	991251	HTI 40	-
ME863/037-1	OBH03	20.01.12	15:53	40°52.563' N	17°52.508' E	105.9 m	040304	HTI 113	-
ME863/038-1	OBH04	20.01.12	16:16	40°54.756' N	17°54.462' E	114.8 m	010403	HTI 39	-
ME863/039-1	OBH05	20.01.12	16:46	40°56.979' N	17°56.323' E	127.2 m	010402	HTI 118	-
ME863/040-1	OBH06	20.01.12	17:11	40°59.207' N	17°58.282' E	176.6 m	010406	HTI 49	-
ME863/041-1	OBH07	20.01.12	17:39	41°01.414' N	18°00.199' E	660.0 m	991256	HTI 64	-
ME863/042-1	OBH08	20.01.12	18:02	41°03.638' N	18°02.131' E	866.0 m	991240	HTI 93	-
ME863/043-1	OBH09	20.01.12	18:27	41°05.848' N	18°04.073' E	975.0 m	991260	HTI 53	-
ME863/044-1	OBH10	20.01.12	18:52	41°08.075' N	18°05.977' E	1030.0 m	991234	HTI 48	-
ME863/045-1	OBH11	20.01.12	19:17	41°10.312' N	18°07.913' E	1058.0 m	801201	HTI 78	-
ME863/046-1	OBH12	20.01.12	19:46	41°12.539' N	18°09.815' E	1074.0 m	090702	HTI 68	-
ME863/047-1	OBH13	20.01.12	20:10	41°14.702' N	18°11.746' E	1083.0 m	000706	HTI 45	-
ME863/048-1	OBH14	20.01.12	20:42	41°16.955' N	18°13.651' E	1092.0 m	991259	HTI 96	-
ME863/049-1	OBH15	20.01.12	21:11	41°19.184' N	18°15.586' E	1093.0 m	991252	HTI 120	-
ME863/050-1	OBH16	20.01.12	21:36	41°21.375' N	18°17.517' E	1106.0 m	040101	HTI 23	-
ME863/051-1	OBH17	20.01.12	22:02	41°23.569' N	18°19.445' E	1110.0 m	010409	HTI 102	-
ME863/052-1	OBH18	20.01.12	22:30	41°25.786' N	18°21.416' E	1113.0 m	040102	HTI 81	-
ME863/053-1	OBH19	20.01.12	23:00	41°27.945' N	18°23.273' E	1089.0 m	061204	HTI 119	-
ME863/054-1	OBH20	20.01.12	23:30	41°30.180' N	18°25.172' E	1084.0 m	991249	HTI 110	-
ME863/055-1	OBH21	20.01.12	23:51	41°32.400' N	18°27.134' E	1052.0 m	991247	HTI 115	-
ME863/056-1	OBH22	21.01.12	00:14	41°34.616' N	18°29.055' E	1013.0 m	050811	HTI 114	-
ME863/057-1	OBH23	21.01.12	01:44	41°36.813' N	18°31.020' E	945.0 m	010404	OAS 15	-
ME863/058-1	OBH24	21.01.12	02:08	41°39.034' N	18°32.853' E	708.0 m	Sercel	OAS 12	-
ME863/059-1	OBS25	21.01.12	02:36	41°41.289' N	18°34.876' E	760 m	991250	HTI 42	Owen 1001-113
ME863/060-1	OBS26	21.01.12	03:09	41°43.494' N	18°36.768' E	335 m	991255	HTI Geomar1	Owen 0509-073
ME863/061-1	OBS27	21.01.12	03:33	41°45.694' N	18°38.632' E	214 m	991258	HTI 51	Owen 1101-114
ME863/062-1	OBS28	21.01.12	03:57	41°47.910' N	18°40.543' E	144 m	991248	HTI 44	Owen 0104-002
ME863/063-1	OBS29	21.01.12	04:25	41°50.145' N	18°42.438' E	241 m	010401	HTI 97	Owen 1001-116
ME863/064-1	OBS30	21.01.12	04:48	41°52.346' N	18°44.445' E	103 m	040807	HTI 38	Owen 34
ME863/065-1	OBS31	21.01.12	05:19	41°54.583' N	18°46.297' E	111 m	991242	HTI 61	Owen 1001-121
ME863/066-1	OBS32	21.01.12	05:49	41°59.774 N	18°48.244 E	98 m	061201	HTI 108	Owen 0509-075
ME863/067-1	OBS33	21.01.12	06:16	41°58.966 N	18°50.199 E	90 m	110101	OAS 37	Owen 1001-120
ME863/068-1	OBS34	21.01.12	06:38	42°01.196 N	18°52.119 E	70 m	991243	OAS HH	Owen 1001-115
ME863/069-1	OBS35	21.01.12	07:00	42°03.444 N	18°54.038 E	70 m	000712	HTI 34	Owen 0104-003
ME863/070-1	OBS36	21.01.12	07:49	42°05.704 N	18°55.927 E	66.5 m	061202	OAS 14	Owen 0708-099

Station	Instrument	deployment					Recorder	Hyd	Geophone
		date	time	lat	lon	depth			
ME863/120-1	OBS40	26.01.12	08:00	42°00.876' N	19°02.205' E	59.2 m	991258	OAS 14	Owen 0708-099
ME863/121-1	OBS41	26.01.12	08:33	42°00.585' N	18°57.377' E	69.0 m	061201	HTI 51	Owen 1001-114
ME863/122-1	OBS42	26.01.12	09:05	42°00.362' N	18°52.594' E	70.3 m	991242	HTI 108	Owen 0509-075
ME863/123-1	OBS43	26.01.12	09:35	42°00.123' N	18°47.795' E	88.0 m	040807	OAS HH	Owen 1001-115
ME863/124-1	OBS44	26.01.12	10:08	41°59.796' N	18°43.021' E	132.7 m	010401	HTI 44	Owen 1001-118
ME863/125-1	OBS45	26.01.12	10:41	41°59.550' N	18°38.226' E	175.7 m	991248	HTI 97	Owen 1001-116
ME863/126-1	OBS46	26.01.12	11:11	41°59.254' N	18°33.433' E	211.0 m	061202	HTI 34	Owen 11
ME863/127-1	OBS47	26.01.12	11:42	41°59.013' N	18°28.616' E	309.0 m	991255	OAS 37	Owen 1001-120
ME863/128-1	OBS48	26.01.12	12:11	41°58.742' N	18°23.817' E	559.0 m	991250	HTI 38	Owen 1001-121
ME863/129-1	OBH49	26.01.12	12:39	41°58,490' N	18°19,010' E	895.0 m	Sercel	HTI 61	
ME863/130-1	OBS50	26.01.12	13:09	41°58.229' N	18°14.217' E	1096.0 m	110101	HTI 42	Owen 1001-113
ME863/131-1	OBS51	26.01.12	13:37	41°57.907' N	18°09.448' E	1178.0 m	000712	HTI 27	Owen 0509-073
ME863/132-1	OBH52	26.01.12	15:??	41°57.652' N	18°04.650' E	1202.0 m	991243	HTI 12	
ME863/133-1	OBH53	26.01.12	14:40	41°57.381' N	17°59.826' E	1205.0 m	010404	OAS 15	
ME863/134-1	OBH54	26.01.12	15:17	41°57.120' N	17°55.071' E	1208.0 m	050811	HTI 114	
ME863/135-1	OBH55	26.01.12	15:43	41°56.847' N	17°50.240' E	1206.0 m	991247	HTI 115	
ME863/136-1	OBH56	26.01.12	16:11	41°56.548' N	17°45.486' E	1207.0 m	991249	HTI 110	
ME863/137-1	OBH57	26.01.12	16:37	41°56.326' N	17°40.458' E	1185.0 m	061204	HTI 119	
ME863/138-1	OBH58	26.01.12	17:04	41°56.026' N	17°35.887' E	1123.3 m	040102	HTI 81	
ME863/139-1	OBH59	26.01.12	17:31	41°55.767' N	17°31.111' E	1092.2 m	010409	HTI 102	
ME863/140-1	OBH60	26.01.12	17:58	41°55.483' N	17°26.327' E	1015.6 m	040101	HTI 23	
ME863/141-1	OBH61	26.01.12	18:24	41°55.246' N	17°21.508' E	1006.2 m	991252	HTI 120	
ME863/142-1	OBH62	26.01.12	18:50	41°54.991' N	17°16.693' E	941.6 m	991259	HTI 96	
ME863/143-1	OBH63	26.01.12	19:18	41°54.740' N	17°11.933' E	875.8 m	040304	OAS 45	
ME863/144-1	OBH64	26.01.12	19:48	41°54.466' N	17°07.112' E	787.3 m	090702	HTI 68	
ME863/145-1	OBH65	26.01.12	20:17	41°54.165' N	17°02.368' E	627.2 m	081201	HTI 78	
ME863/146-1	OBH66	26.01.12	20:47	41°53.900' N	16°57.519' E	535.6 m	050810	HTI 109	
ME863/147-1	OBH67	26.01.12	21:18	41°53.659' N	16°52.731' E	332.7 m	991260	HTI 53	
ME863/148-1	OBH68	26.01.12	21:48	41°53.372' N	16°47.942' E	188.4 m	991240	HTI 93	
ME863/149-1	OBH69	26.01.12	22:19	41°53.081' N	16°43.164' E	139.8 m	991256	HTI 64	
ME863/150-1	OBH70	26.01.12	22:48	41°52.810' N	16°38.376' E	119.2 m	010406	HTI 49	
ME863/151-1	OBH71	26.01.12	23:24	41°52.546' N	16°33.602' E	102.2 m	010402	HTI 118	
ME863/152-1	OBH72	26.01.12	23:56	41°52.308' N	16°28.771' E	86.6 m	010403	OAS 21	
ME863/153-1	OBH73	27.01.12	00:25	41°52.057' N	16°23.961' E	67.3 m	040602	OAS 35	
ME863/154-1	OBH74	27.01.12	00:55	41°51.749' N	16°19.178' E	38.5 m	991251	HTI 40	
ME863/155-1	OBH75	27.01.12	01:18	41°51.620' N	16°16.873' E	20.2 m	040803	HTI 116	

Station	Instrument	deployment					Recorder	Hyd	Geophone
		date	time	lat	lon	depth			
ME863/070-1	OBS36	21.01.12	07:49	42°05.704' N	18°55.927' E	66.5 m	061202	OAS 14	Owen 0708-099
ME863/110-1	OBS37	24.01.12	15:13	42°07.945' N	18°58.537' E	55.0 m	991258	HTI 51	Owen 1001-114
ME863/112-1	OBS38	25.01.12	04:26	42°01.860' N	19°06.485' E	35.0 m	020503	OAS HH	Owen 1001-115
ME863/113-1	OBS39	25.01.12	04:45	42°03.281' N	19°04.606' E	46.0 m	061201	HTI 80	Owen 0509-075

8 Data and Sample Storage and Availability

The bathymetry data were transferred to the BSH immediately after the cruise.

The seismic and hydro-acoustic raw data as well as processed seismic data are archived on a dedicated server at GEOMAR, which is daily backed up and which holds all data since the founding days of GEOMAR. Other data generated during modeling work, e.g. from seismic wide-angle and seismological analyses, will be stored in the GEOMAR data management system after publication, but latest at the end of the project. Contact person is Professor Dr. H. Kopp at GEOMAR, Kiel.

The GEOMAR system is connected with AWI's PANGAEA data base in Bremerhaven, which provides long-term archival and access to the data. The data are globally searchable, and links to the data owners will provide points of contact to project-external scientists. Data will be publicly available October 2014.

9 Acknowledgements

We sincerely thank Cpt. Schwarze and his crew for their professional assistance at sea. The ALPHA cruise is funded through the Deutsche Forschungsgemeinschaft DFG. The authors wish to express their gratitude to L. Improta and C. Chiarabba (INGV Rome), B. Schurr (GFZ Potsdam), B. Glavatovic (Seismological Observatory of Montenegro), L. Duni (Polytechnic Univ. Tirana), M. Herak (Univ. Zagreb) and all other colleagues who have supported our work onshore and offshore.

10 References

Anderson, H. and Jackson, J., 1987. Active tectonics of the Adriatic Region. Geophysical Journal of the Royal Astronomical Society, 91, 937-983.

Argnani, A., Favali, P., Frugoni, F., Gasperini, M., Ligi, M., Marani, M., Mattietti, G., and Mele, G., 1993. Foreland deformational pattern in the southern Adriatic Sea. Annali di Geofisica, v. 36, p. 229–247.

Argnani A., Rovere M. and Bonazzi C., 2009. Tectonics of the Mattinata Fault offshore south Gargano (southern Adriatic Sea, Italy): implications on active deformation in the foreland of the Southern Apennines. G.S.A. Bull., 121, 1421-1440.

Babbucci, D., Tamburelli, C., Viti, M., Mantovani, E., Albarello, D., D'Onza, F., Cenni, N. and Mugnaioli, E., 2004. Relative motion of the Adriatic with respect to the confining plates: seismological and geodetic constraints. Geophysical Journal International, 159, 765-775.

Battaglia, M., Murray, M.H., Serpelloni, E. and Bürgmann, R., 2004. The Adriatic region: An independent microplate within the Africa-Eurasia collision zone. Geophysical Research Letters, 31, L09605, doi:10.1029/2004GL019723.

Benetatos, C. and Kiratzi, A., 2006. Finite-fault slip models for the 15 April 1979 (Mw 7.1) Montenegro earthquake and its strongest aftershock of 24 May 1979 (Mw 6.2). Tectonophysics, 421, 129-143.

Bennett, R.A., Hreinsdóttir, S., Buble, G., Bašić, T., Bačić, Ž., Marjanović, M., Casale, G., Gendaszek, A. and Cowan, D., 2008. Eocene to present subduction of southern Adria mantle lithosphere beneath the Dinarides. Geology, 36, 3-6.

Burchfiel, B.C., Nakov, R., Dumurdzanov, N., Papanikolaou, D., Tzankov, T., Serafimovski, T., King, R.W., Kotzev, V., Todosov, A. and Nurce, B., 2008. Evolution and dynamics of the Cenozoic tectonics of the South Balkan extensional system. Geosphere, 4, 919-938.

Caporali, A., Aichhorn, C., Barlik, M., Becker, M., Fejes, I., Gerhatova, L., Ghitau, D., Grenerczy, G., Hefty, J., Krauss, S., Medak, D., Milev, G., Mojzes, M., Mulic, M., Nardo, A., Pesec, P., Rus, T., Simek, J., Sledzinski, J., Solaric, M., Stangl, G., Stopar, B., Vespe, F. and Virag, G., 2009. Surface kinematics in the

Channell, J.E.T. and Horváth, F., 1976. The African/Adriatic promontory as a paleogeographical premise for Alpine orogeny and plate movements in the Carpatho-Balkan region. Tectonophysics, 35, 71-101.

Console, R. and Favali, P., 1981. Study of the Montenegro earthquake sequence (March - July 1979). Bulletin of the Seismological Society of America, 71, 1233-1248.

Copley, A., Boait, F., Hollingsworth, J., Jackson, J. and McKenzie, D., 2009. Subparallel thrust and normal faulting in Albania and the roles of gravitational potential energy and rheology contrasts in mountain belts. J. Geophys. Res., 114, doi 10.1029/2008JB005931.

Cvetković, V., Prelević, D., Downes, H., Jovanović, M., Vaselli, O. and Pecskay, Z., 2004. Origin and geodynamic significance of Tertiary postcollisional basaltic magmatism in Serbia (central Balkan Peninsula). Lithos, 73, 161-186.

D'Agostino, N., Avallone, A., Cheloni, D., D'Anastasio, E., Mantenuto, S. and Selvaggi, G., 2008. Active tectonics of the Adriatic region from GPS and earthquake slip vectors. J. Geophys. Res., 113.

Davison I., Alsop I., Evans N.G. and Safaricza M., 2000. Overburden deformation patterns and mechanisms of salt diapir penetration in the Central Graben, North Sea. Mar. Petrol. Geol., 17, 601-618.

De' Dominiciis A. and Mazzoldi G., 1987. Interpretazione geologico-strutturale del margine orientale della piattaforma Apula. Mem. Soc. Geol. It., 38, 163-176.

Di Stefano, R., E. Kissling, C. Chiarabba, A. Amato, and D. Giardini (2009): Shallow subduction beneath Italy: Three-dimensional images of the Adriatic-European-Tyrrhenian Lithosphere system based on high quality P wave arrival times. J. Geophys. Res., doi:10.1029/2008JB005641.

Dumurdzanov, N., Serafimovski, T. and Burchfiel, B.C., 2005. Cenozoic tectonics of Macedonia and its relation to the South Balkan extensional regime. Geosphere, 1, 1-22.

Flueh, E. R. and Bialas, J. A digital, high data capacity ocean bottom recorder for seismic investigations. Int. Underwater Systems Design, 18(3):18–20, 1996.

Flueh, E. R. and Bialas, J.Ocean Bottom Seismometers.Sea Technology, 40(4):41–46, 1999.

Grenerczy, G., Sella, G., Stein, S. and Kenyeres, A., 2005. Tectonic implications of the GPS velocity field in the northern Adriatic region. Geophys. Res. Lett., 32, L16311, doi:10.1029/2005GL022947.

Handy, M.R., M. Schmid, S., Bousquet, R., Kissling, E. and Bernoulli, D., 2010. Reconciling plate-tectonic reconstructions of Alpine Tethys with the geological-geophysical record of spreading and subduction in the Alps. Earth-Science Reviews, 102, 121-158.

Herak, M. (1991): Dinarides, Mobilistic view of the Genesis and Structure. Acta Geologica, 21(2), 1- 83.

Jolivet, L. and Brun, J.-P., 2010. Cenozoic geodynamic evolution of the Aegean. International Journal of Earth Sciences, 99, 109-138.

Lister, G.S., Banga, G., Feenstra, A., 1984. Metamorphic core complexes of cordilleran type in the Cyclades, Aegean Sea, Greece. Geology 12, 221–225.

Moretti I. and Royden L., 1988. Deflection, gravity anomalies and tectonics of doubly subducted continental continental lithosphere – Adriatic and Ionian Seas. Tectonics 7, 4, 875-893.

Nicolai, C. and Gambini, R. 2007. Structural architecture for the Adria platform-and-basin system, Bollettino della Societa Geologica Italiana, Volume speciale, ISSN 1722-2818.

Oldow, J., Ferranti, L., Lewis, D.S., Campbell, J.K., D'Argenio, B., Catalano, R., Pappone, G., Carmignani, L., Conti, P. and Aiken, C.L.V., 2002. Active fragmentation of Adria, the north African promontory, central Mediterranean orogen. Geology, 30, 779–782.

Pamić, J., 1993. Eoalpine to Neoalpine magmatic and metamorphic processes in the northwestern Vardar Zone, the easternmost Periadriatic Zone and the southwestern Pannonian Basin. Tectonophysics, 226, 503-518.

Pamić, J., 2002. The Sava-Vardar Zone of the Dinarides and Hellenides versus the Vardar Ocean. Eclogae Geologicae Helvetiae, 95, 99-113.

Piromallo, C. and Morelli, A., 2003. P wave tomography of the mantle under the Alpine-Mediterranean area. Journal of Geophysical Research, 108 (B2), doi:10.1029/2002JB001757.

Schefer, S., Cvetković, V., Fügenschuh, B., Kounov, A., Ovtcharova, M., Schaltegger, U. and Schmid, S., 2011. Cenozoic granitoids in the Dinarides of southern Serbia: age of intrusion, isotope geochemistry, exhumation history and significance for the geodynamic evolution of the Balkan Peninsula. International Journal of Earth Sciences, 100, 1181–1206, doi: 10.1007/s00531-010-0599-x.

Schmid, S.M., Bernoulli, D., Fügenschuh, B., Matenco, L., Schuster, R., Schefer, S., Tischler, M. and Ustaszewski, K., 2008. The Alpine-Carpathian-Dinaridic orogenic system: correlation and evolution of tectonic units. Swiss Journal of Geosciences, 101, 139-183.

Scisciani, V. and Calamita, F. (2009): Active intraplate deformation within Adria: Examples from the Adriatic region, Tectonophysics, 476, 57-72.

Šumanovac, F., Orešković, J., Grad, M. and the A.L.P. Working Group, 2009. Crustal structure at the contact of the Dinarides and Pannonian basin based on 2-D seismic and gravity interpretation of the Alp07 profile in the ALP 2002 experiment. Geophysical Journal International, 179, 615-633.

Ustaszewski, K., Schmid, S.M., Fügenschuh, B., Tischler, M., Kissling, E., Spakman, W.A., (2008). A map-view restoration of the Alpine-Carpathian-Dinaridic system for the Early Miocene. Swiss J. Geosci. 101, Supplement 1, 273–S294, DOI 10.1007/s00015-008-1288-7.

Ustaszewski, K., Kounov, A., Schmid, S.M., Schaltegger, U., Krenn, E., Frank, W. and Fügenschuh, B., 2010. Evolution of the Adria-Europe plate boundary in the northern Dinarides: From continent-continent collision to back-arc extension. Tectonics, 29, TC6017, doi:10.1029/2010TC002668.

Vannucci, G., Pondrelli, S., Argnani, A., Morelli, A., Gasperini, P., and Boschi, E., 2004. An atlas of Mediterranean seis- micity: Annali di Geofisica, vol. 47, suppl., p. 247–306.

Velaj T., Davison I., Serjani A. and Alsop I., 1999. Thrust tectonics and the role of evaporites in the Ionian Zone of the Albanides. AAPG Bull., 83, 1408-1425.

Venisti N., G. Calcagnile, A. Pontevivo, and G.F. Panza (2005): Tomographic study of the Adriatic Plate. Pure and Appl. Geophys., 162, 311-329.

Wortmann, U. G., H. Weissert, H. Funk, and J. Hauck (2001): Alpine plate kinematics revisited: The Adria problem, Tectonics, 20, 134 – 147, doi:10.1029/2000TC900029.

Yanev, Y. and J.M. Bardintzeff (1997): Petrology, volcanology and metallogeny of Palaeogene collision-related volcanism of the Eastern Rhodopes (Bulgaria). Terra Nova, 9, 1-8.